Field Theory and Renormalization Group for the Magnetocaloric Effect

Quantum Fields and Fundamental Forces (MSc)
Jacob Craigie
Department of Physics
Imperial College London
SW7 2BZ

Supervisor: Prof. Dimitri Vvedensky

Abstract

In this thesis, we will first review the physics of the magnetocaloric effect (MCE), and the giant magnetocaloric effect (GMCE), with a brief review of the statistical mechanics techniques we will need throughout. Then we will review the state of our understanding of the GMCE through the use of compressible Ising models, examining the central theoretical models (Domb [1], Bean-Rodbell [2], Baker-Essam [3], etc...). Finally we will attempt to apply renormalization group (RG) and field theory techniques to the compressible Ising model for the MCE/GMCE.

This dissertation is primarily concerned with theoretical aspects, and hence we only briefly mention material concerns, and entirely skip over experimental setups etc... (though for such concerns, [4–10] may be a good starting point).

London, September 2012

Submitted in partial fulfillment of the requirements for the degree of Master of Science of Imperial College London

Acknowledgements

Firstly I would like to thank my fiancé, for being my fiancé despite my absent minded state while I worked on this dissertation.

I would also like to thank Professor Dimitri Vvedensky for agreeing to be my supervisor, and providing we with an ideal dissertation topic. I feel I am only just beginning to explore the depths of the physics involved!

Also, I would like to thank the lecturers of my courses this year, for guiding me in exploring these fascinating topics.

And of course thank you to my parents, for being there always.

Contents

1 Background

1.1 Introduction

First, we must review the magnetocaloric effect (MCE), giant magnetocaloric effect (GMCE) and aspects of statistical mechanics and field theory that we will need throughout.

1.2 Magnetocaloric Effect

The MCE is a reversible magneto-thermodynamic process that forms the basis for the magnetic cooling cycle (Fig. 1.2), a promising alternative to the conventional vapor-cycle refrigeration, that may soon be viable for commercial and domestic applications [11]. The effect was discovered in pure iron by Emil Warburg (1880) with a cooling effect in the range of $0.5 - 2.0KT^{-1}$, the first working prototypes being constructed in 1933.

Magnetic cooling technology would be more energy efficient ($\sim$60% efficiency compared to $\sim$15% efficiency for vapor-cycle cooling) and less polluting, with a considerably smaller carbon footprint than traditional cooling technology. Ozone depleting chemicals, hazardous chemicals and greenhouse gases are not needed, the only liquids present are non-volatile heat exchange media. Unfortunately, currently available materials only reach such efficiency in high magnetic fields of $\sim$5T, much higher than can be created conveniently for domestic applications etc... With refinement, the MCE may be used to reach extremely low temperatures, as well as the ranges used in everyday commercial applications like fridges, depending on the design of the system.

The search is on to find better magnetocaloric materials and break down the barriers to application, with recent developments in room temperature magnetic refrigeration [12], progress is being made [13, 14] (and see [15] for a detailed review of the theory and properties of known MCE materials). There exists several magnetic cooling prototypes around the world, with a recent upsurge in related publications. However, advances in our theoretical understanding are also necessary.

We will begin by understanding the MCE from a theoretical perspective. We consider a magnetocaloric material, modeled as a magnetic lattice thermally coupled to a crystal

lattice. Initially, considering just the magnetic degrees of freedom: the material is at ambient temperature $T_{initial}$ above the materials Curie temperature, $T_{initial} > T_c$; there is no external magnetic field, $\vec{H}_{ext} = \vec{0}$; and the electron magnetic moments at each site are not aligned (Fig. 1.1a).

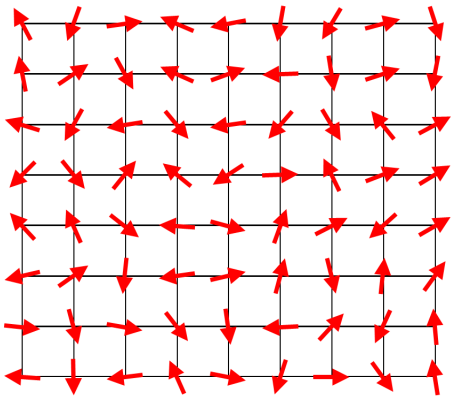

(a) At $T > T_c$, with no external magnetic field $\vec{H}_{ext} = \vec{0}$. The spins are not aligned, i.e. there is no correlation between sites on the lattice.

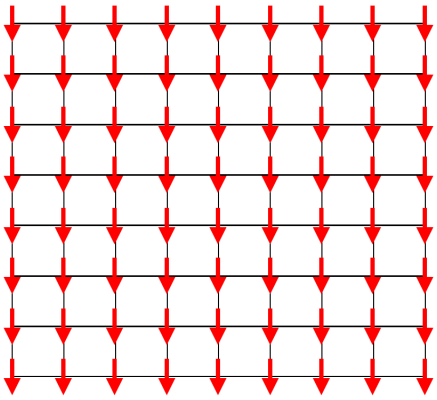

(b) At high external magnetic field $\vec{H}_{ext}$, with reduced temperature. Eventually the alignment may become saturated, all the spins point in the same direction.

Figure 1.1: Regular 2-dimensional lattice of spins (magnetic moments), each spin is allowed to point in any direction within the plane, with a fixed magnitude.

Applying an external magnetic field, $\vec{H}_{ext}$, aligns the electron spins, reducing the magnetic entropy. As the magnetic field is increased, and the temperature is reduced, the spins become more and more aligned, eventually the alignment is saturated and all the spins point in the same direction (Fig. 1.1b).

1.2.1 Adiabatic Cycle

If the magnetization is done adiabatically, the laws of thermodynamics dictate that the total entropy of the system (spin and lattice degrees of freedom) must be constant, as in a reversible process. Hence the entropy lost from the magnetic degrees of freedom must be absorbed by other degrees of freedom in the material, in this case, by the lattice degrees of freedom. As the lattice entropy increases, the material heats up to a temperature T_{final}:

$$T_{final} = T_{initial} + \Delta T^{0 \to H}_{adiabatic}, \tag{1.1}$$

where $\Delta T^{0 \to H}_{adiabatic}$ is the temperature change of the material as the external magnetic field $\vec{H}_{ext}$ is increased from $\vec{0}$ to $\vec{H}$.

This heat is carried away to the ambient atmosphere by heat transfer, returning the material to its starting temperature $T_{initial}$, but now magnetized. Finally, the material is isolated again, and the magnetic field is adiabatically removed so that the total entropy remains constant. The agitating action of the thermal energy (phonons) causes the magnetic moments to randomize again, entropy is redistributed among magnetic and lattice degrees of freedom, and hence the material chills to a temperature below is starting temperature:

$$T_{final} = T_{initial} - \Delta T^{0 \to H}_{adiabatic}. \tag{1.2}$$

The material can now brought back to the ambient temperature $T_{initial}$ by heat exchange with the material being refrigerated - heat energy is transfered from the material being refrigerated to the magnetocaloric material. We have achieved a cycle whereby the magnetic material has been returned to its original temperature and magnetization, and heat has been transferred from the heat load to its surroundings. Assuming any thermal hysteresis loss from the heating/cooling cycle can be neglected, the cycle is reversible and can be repeated for further cooling.

The MCE is intrinsic to particular materials. Currently, some of the most promising materials, providing the biggest entropy change at near room temperature are seen in gadolinium and its alloys, i.e. GdDy, GdTb, etc... Research is focused on increasing the temperature change and making the process more practicable, i.e. as the temperature change is increased, weaker magnetic fields and less material may be used.

1.2.2 Isothermal Cycle

If the magnetization and demagnetization is done isothermally, the magnetocaloric effect corresponds to the isothermal entropy change $\Delta S_M^{0\to H}$, where the heat exchange is proportional to the magnetic entropy change:

$$\Delta Q = T\Delta S_M^{0\to H}. \tag{1.3}$$

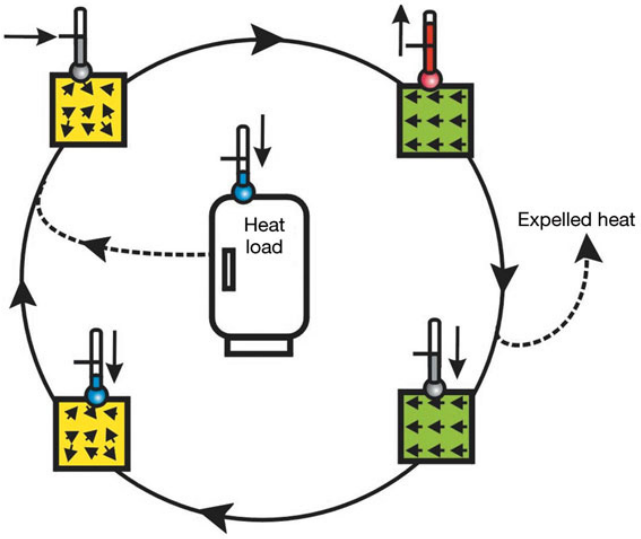

Figure 1.2: Diagram of magnetic refrigeration cycle, which transports heat from the heat load to the surroundings. Yellow shows the material without magnetic field, and green shows the material with high magnetic field. Image taken from [16].

1.2.3 Cycle Optimization

To break down the barriers to application of the MCE, it is necessary to increase the effect as much as possible. Hence, it is interesting to examine the thermodynamic limits [17] of the MCE for a 1st order phase transition model so that we may compare available materials, and investigate how to bring them to their full potential, through optimization at all scales.

Of course, optimization of the cycle requires optimizing the structure of the material at all scales, examining the material properties, investigating effects of isotropy etc... as well as optimizing the experimental setup composed of pumps, electric motors, secondary fluids, heat exchangers etc... which all have their associated inefficiencies. However, here we will only concern ourselves with the fundamental thermodynamic limits, and leave the synthesis and microstructuring to the experimentalists.

Magnetic phase transitions can be conveniently described by the following two magnetothermal properties: the isothermal entropy change of the entire material ΔS, or the adiabatic temperature change $\Delta T_{adiabatic}^{0\to H}$ as the magnetic field is increased from $\vec{0}$ to $\vec{H}$.

In order to maximize the temperature change $\Delta T_{adiabatic}^{0\to H}$, we wish to maximize the magnetic entropy change on magnetization. The entropy change due to the applied magnetic field is enhanced by choosing a "working temperature" of the material close to a field-induced 1$^{\text{st}}$ order phase transition critical temperature T_c, i.e. a ferromagnetic low temperature (FM) to high-temperature paramagnetic (PM) critical point.

We wish to calculate the magnetic entropy change as a function of the temperature T and magnetic field H, ie. $\Delta S_M(T,H)$. We begin by considering the Maxwell relation for magnetic entropy:

$$\left(\frac{\partial S_M(T,H)}{\partial H}\right)_T = \left(\frac{\partial M(T,H)}{\partial T}\right)_H, \tag{1.4}$$

where M is the total magnetization. We note that magnetic entropy dependence on field is maximized at at critical point $T \sim T_c$, hence maximizing the left hand side of the equation.

Rearranging and integrating Eq. (1.4), where we are interested in the magnetic entropy S_M (neglecting other degrees of freedom the material may have that carry entropy) we obtain:

$$\Delta S_M(T,H) = S_M(T,H) - S_M(T,0) = \int_0^H \left(\frac{\partial M}{\partial T}\right)_{H'} \mathrm{d}H', \tag{1.5}$$

for the isothermal cycle.

For the adiabatic cycle, we obtain [18] a change in temperature $\Delta T_{adiabatic}$:

$$\Delta T_{adiabatic}(T,H) = \int_0^H \frac{T}{C_p(T,H)} \left(\frac{\partial M}{\partial T}\right)_H \mathrm{d}H'. \tag{1.6}$$

Theoretical Limit of $\Delta T_{adiabatic}$

We wish to know the theoretical limits of the adiabatic temperature change $\Delta T_{adiabatic}$ in Eq. (1.6).

Several authors have shown, by considering the maximum possible $\Delta T_{adiabatic}$ near a Curie transition [19], and assuming that within a small temperature interval, $(\partial M/\partial T)|_H$ is constant, the optimum value of $\Delta T_{adiabatic}$ is

$$\Delta T_{adiabatic}^{optimal} = \left(\frac{M_{sat} T H_{max}}{C_p}\right)^{\frac{1}{2}}, \tag{1.7}$$

where M_{sat} is the saturation magnetization, H_{max} is the maximum field, and C_p is the heat capacity of the material.

1.3 Ising Model

We briefly refresh our knowledge of the Ising model, which we will later adapt to the MCE/GMCE.

The Ising model is a central paradigm in physics, and has immense depth, and applicability to a vast array of problems ranging from the familiar ferromagnetism and phase transitions to statistical finance, econophysics, agent based systems and market behavior [20].

The Ising model was originally developed in the 1920's as a model for ferromagnetism. It models a ferromagnet as a d-dimensional regular lattice of (classical) spins, which may point either up, $\uparrow, +1$, or down, $\downarrow, -1$. The lattice parameter, a, is the spacing between each spin. The model is particularly useful for us, in that it shows a phase transition from a ferromagnetic to paramagnetic state at some temperature T_c, in fact the 2-dimensional Ising model on a square lattice is one of the simplest systems showing such a phase transition.

A discrete two-state variable, $\sigma_j \in \{+1, -1\}$, called the spin, describes the state of each lattice site, labeled by j. Nearest neighbor sites interact with an exchange interactions strength J (that may be taken to vary from site to site). We may also consider a constant external magnetic field H interacting with each of the sites. The total energy of the system is described by the Hamiltonian:

$$\mathbf{H} = -J \sum_{<i,j>} \sigma_i \cdot \sigma_J - H \sum_i \sigma_i, \tag{1.8}$$

where the first term on the right hand side is the energy of exchange interaction (the sum being taken only over nearest neighbors, with each nearest neighbor pair being counted only once), and the second term is the energy of interaction with the external magnetic field. Note that, if $J > 0$, the energy is minimized for aligned spins, and hence the interaction is ferromagnetic (vice versa for $J < 0$, the interaction is anti-ferromagnetic). Also the minus sign before the external magnetic field H term means that the energy is minimized for spins aligned with the field.

From the Boltzmann distribution, in the canonical ensemble, we obtain the probability for the system to be in any particular configuration σ at equilibrium:

$$P(\beta, \sigma) = \frac{e^{-\beta \mathbf{H}(\sigma)}}{Z_\beta}, \tag{1.9}$$

where β is the inverse temperature $\beta = 1/(k_B T)$, k_B is the Boltzmann constant, and $Z(\beta)$ is the partition function:

$$Z(\beta) = \sum_\sigma e^{-\beta \mathbf{H}(\sigma)}, \tag{1.10}$$

the sum being taken over the 2^N possible spin configurations (N being the total number of sites).

At low temperatures, there exists complete magnetization with all spins aligned, and perfect ferromagnetic long range order. As a ferromagnet is heated from below the critical point, the thermal energy overcomes the exchange interactions, destroying the order. Magnetization decreases continuously, vanishing at the Curie temperature T_c, at which a change of phase occurs to a paramagnetic state above T_c. This is not a 1^{st} order

phase transition since the entropy (a first order derivative) changes continuously, but a discontinuity is observed in the specific heat (a second order derivative) at T_c.

1d Ising model

The 1-dimensional Ising model has no phase transition, and was solved by Ising himself in 1925. He proved that (see any statistical mechanics textbook, i.e. [21]), given a 1-dimensional periodic lattice of N sites, with the Hamiltonian, Eq. (1.8) above, the free energy density (per site) is:

$$f(\beta, H) = -\lim_{N\to\infty} \frac{1}{\beta N} \ln Z(\beta) \tag{1.11}$$

$$= -\frac{1}{\beta} \ln \left[e^{\beta J} \cosh \beta H + \sqrt{e^{2\beta J} (\sinh \beta H)^2 + e^{-2\beta J}} \right], \tag{1.12}$$

where the partition function Z_N is:

$$Z_N = e^{N\beta J} \left(\left[\cosh \beta H + \sqrt{\sinh^2 \beta H + e^{-4\beta J}} \right]^N + \left[\cosh \beta H - \sqrt{\sinh^2 \beta H + e^{-4\beta J}} \right]^N \right). \tag{1.13}$$

For the $H = 0$ case, we wish to see if there is a spontaneous phase transition from high temperature unordered paramagnetic state, to a low temperature ordered ferromagnetic state. The spin-spin correlation between sites i and $i + n$ can be calculated:

$$\langle \sigma_i \sigma_{i+n} \rangle = e^{n \ln(\tanh K)} \equiv e^{-n/\xi}, \tag{1.14}$$

where $K = \beta J$, $\langle \cdots \rangle$ denotes a thermal average at a temperature T, and we identify the correlation length ξ as

$$\xi = -\frac{1}{\ln(\tanh K)}. \tag{1.15}$$

Since $\tanh K < 1$, then $\xi > 0$, and the correlation function decays exponentially with inreasing n at non-zero temperatures. At low temperatures (high K), we have

$$\ln(\tanh K) \simeq -e^{-2K}, \tag{1.16}$$

and hence

$$\xi \simeq e^{2K} = e^{2J/k_B T}, \tag{1.17}$$

and so the correlation length diverges as $T \to 0$, thus there is no phase transition above $T = 0$, the correlated ferromagnetic state is only reached at $T = 0$, i.e. the Curie temperature is $T_c = 0$. In fact, when Ising originally discovered this solution, he concluded the model was incorrect for ferromagnetism, as it was missing the essential phase transition at non-zero T_c.

As the correlation length diverges, the alignment of a single spin can spread throughout the system - the state of the system can be totally changed by a small perturbation. Diverging correlation lengths are a central feature of systems undergoing a continuous phase change.

Other thermodynamic quantities, such as C_v (heat capacity at constant volume), M, χ (magnetic susceptibility), U (total energy) etc... can all be obtained from the partition function Z and free energy F by taking appropriate derivatives.

2d Ising model

The 2-dimensional, regular square lattice Ising model proved to be much more complicated, an analytic solution, known as Onsager's solution, being eventually discovered in 1944. In contrast to the 1-dimensional case, Onsager's solution shows that the 2-dimensional Ising model does have a spontaneous ferromagnetic phase transition at non-zero temperature. He obtained for the magnetization M as a function of temperature T:

$$M(T) = \left(1 - \left[\sinh\left(\log\left(1+\sqrt{2}\right)\frac{T_c}{T}\right)\right]^{-4}\right)^{\frac{1}{8}}, \tag{1.18}$$

where:

$$T_c = \frac{2J}{\log\left(1+\sqrt{2}\right)}. \tag{1.19}$$

With this solution, it became apparent that ferromagnetic-paramagnetic phase transitions could in-fact be described by the Ising model.

3d Ising model

In 3 dimensions, it is generally thought to be unsolvable. However, it has been show that the 3-dimensional Ising model may be transformed into a representation in terms of non-interacting Fermionic lattice strings which may offer some information. There are also approximate solutions available, some quite precise, i.e. series expansions [22], renormalization group calculations [23], ϵ-expansions [24, 25], Monte Carlo renormalization group calculations [26–28], and Monte Carlo simulations [29].

4d Ising model and above

In 4 dimensions and above, the mean field approach becomes exact, and hence a well understood method exists to calculate behavior around the critical point.

It was also noted by Kenneth Wilson that the 4d Ising model corresponds to the renormalization behavior of the scalar ϕ^4 theory.

1.4 Critical Phenomena

Critical phenomena capture the physics of critical points, which are characterized by particular phenomena such as divergence of correlation length and fractal (scale invariant/conformal) physics. Phase transitions are characterized by sudden changes in the macroscopic properties of a system as the temperature is varied. 1^{st} order phase transitions have a finite jump in the total energy U at the transition temperature - corresponding to the latent heat. Continuous phase transitions have zero latent heat, and no sudden changes in microscopic variables such as the magnetization, however derivative quantities may show divergences. These phenomena can be illustrated through the Ising model.

Consider a simple Ising model, at a certain temperature, without external magnetic field. The energy is given by the classic Ising Hamiltonian:

$$\mathbf{H} = -J \sum_{<i,j>} \sigma_i \cdot \sigma_J, \tag{1.20}$$

where the sum is taken only over nearest neighbor pairs, and J is the constant exchange interaction coupling constant between sites. At high enough temperatures, the thermal energy overcomes the exchange interaction, hence the sites are uncorrelated, and the material is in a paramagnetic state. As the material is cooled to below what is called the Curie temperature, T_c, ferromagnetic long range order takes over, and the spins begin to show correlation. Eventually as the temperature is lowered further, the spins become completely aligned, and the magnetization is saturated. Below the Curie temperature, the remaining clusters of non-aligned spins give us a natural length scale, called the correlation length, ξ. As the Curie temperature is reached from below, these non-aligned clusters grow clusters within themselves, and the correlation length ξ diverges at T_c. The system at T_c, becomes fractal, with non-aligned clusters on all possible length scales, and hence there is no global magnetization.

Above the Curie temperature, the system does not show global ferromagnetic order, however there exists clusters of order, whose size is again called the correlation length. These ordered clusters are destroyed with increasing temperature - the correlation length decreases. Eventually, at infinite temperature, the correlation length falls to zero, and the system is fully disordered.

The Critical Point

At the critical point, $T \to T_c$, the correlation length diverges, $\xi \to \infty$, this presents no physical problem, however certain derived properties diverge, i.e. the susceptibility.

To see this, imagine applying a very small magnetic field to the system at the scale invariant critical point, causing a small perturbation by magnetizing the smallest clusters. However, since clusters exist at all possible scales, this smallest cluster may then magnetize a slightly larger cluster, which may then magnetize another slightly larger cluster etc... until the entire system has been affected. We see that the critical system is highly sensitive and unstable to small perturbations - the original small magnetic field has created a small perturbation, which grew until it affected the entire material, and hence the susceptibility has diverged.

Other properties that are derived from the correlation length may also diverge at the critical point.

A beautiful demonstration of this can be seen in the phenomena of critical opalescence (see Youtube for videos), whereby a transparent liquid undergoes a continuous 2^{nd} order phase transition to a gas state. As the critical point is approached, density fluctuations occur across a wider and wider range of scales. At some point, density fluctuations begin to occur at sizes comparable to the wavelength of visible light, hence scattering light and causing the liquid to appear cloudy. This opalescence is maintained right up to the critical point, demonstrating the fluctuations across all scales remain at the critical point.

Critical Exponents in Magnetism

Let us define reduced variables (where we have set permeability $\mu = 0$):

$$t = \frac{T - T_c}{T_c}, \quad h = \frac{H}{k_B T_c}. \tag{1.21}$$

Approaching the critical point, $h = 0, t = 0$, it can be shown [21] that certain derived quantities diverge as a power law for some exponent, known as the "critical exponents". For example:

$$M(T) \propto t^{\beta}, \quad \chi(T) \propto t^{-\gamma}, \quad M(H) \propto h^{1/\delta}, \tag{1.22}$$

Where the critical exponents are β for $M(T)$, γ (without the minus sign by convention) for $\chi(T)$ and $1/\delta$ for $M(H)$. These critical exponents may be observed experimentally, and it is intriguing to note that often the same set of critical exponents may be observed for very different physical systems - this phenomena is knows as "universality", and may be explained by the renormalization group, which is the main mathematical tool used when studying critical points.

1.5 Mean Field Theory for the Ising Model

Mean field theory is particularly useful to describe the Ising model in dimensions of 4 or greater, where it becomes exact.

The mean field theory replaces the exact interactions by a locally varying mean field. The mean field, as its name suggests, is an average of a region of spins, which varies from site to site as new spins enter the region being averaged and old spins leave. This reduces the amount of spins we need to take into account when calculating, as an interaction between a spin and its neighbors is determined by the average spin of the neighbors, and not the spins individually.

The down side to this approach is that we neglect fluctuations on short scales - one spin can no longer directly influence its neighbor, it must do so through the mean field create by all its neighbors. However it is still possible to identify distinct phases.

In our case, take an Ising model on a d-dimensional regular lattice, with the Hamiltonian given in Eq. (1.8). The magnetization per site is:

$$m = \frac{M}{N} = \frac{1}{N} \left\langle \sum_i \sigma_i \right\rangle = \frac{1}{N} \sum_i \langle \sigma_i \rangle. \tag{1.23}$$

We now express the sum over nearest neighbors in the Hamiltonian Eq. (1.8), as

$$\begin{aligned} \sigma_i \cdot \sigma_j &= (\sigma_i - m + m)(\sigma_j - m + m) \\ &= m^2 + m(\sigma_i - m) + m(\sigma_j - m) + (\sigma_i - m)(\sigma_j - m). \end{aligned} \tag{1.24}$$

The mean-field approximation neglects the last term on the right hand side of this equation, leaving us

$$\sigma_i \cdot \sigma_j \simeq m^2 + m(\sigma_i - m) + m(\sigma_j - m) = -m^2 + m(\sigma_i + \sigma_j). \tag{1.25}$$

The final term represented deviations of nearest neighbor spins from the mean, therefore the mean-field theory neglects fluctuations on short scales. Hence the mean-field approximation to the Hamiltonian is

$$\mathbf{H}_{MF} = -\frac{1}{2}J \sum_{<i,j>} \left[-m^2 + m(\sigma_i + \sigma_j)\right] - H \sum_i \sigma_i. \tag{1.26}$$

The sum can be carried out to give the mean-field approximation to the total energy of the Ising model as:

$$\mathbf{H}_{MF} = \frac{1}{2}NJzm^2 - (Jzm + H) \sum_i \sigma_i, \tag{1.27}$$

the first term being the constant contribution from the average magnetization associated with each site. From this we can obtain the mean-field partition function:

$$Z = e^{-\frac{1}{2}NKzm^2} \left[2\cosh(Kzm + L)\right]^N, \tag{1.28}$$

where $L = \beta H$, and $z = 2d$.

Using this general mean-field procedure, we have obtained the mean-field Hamiltonian and partition function for the Ising model. We can now go on and obtain the Helmholtz free energy $F = -k_B T \ln Z$, magnetization per site m, susceptibility χ etc... by taking appropriate derivatives. In this case, for $H = 0$, we would obtain (after some standard manipulations), for $T < T_c$:

$$m^2 = 3\left(\frac{T^2}{T_c^3}\right)(T_c - T), \tag{1.29}$$

where $T_c = Jz/k_B$. Hence we extract the power law:

$$m \sim (T_c - T)^{1/2}. \tag{1.30}$$

And so we see that the magnetization $m \to 0$ as $T \to T_c$ with critical exponent $\beta = 1/2$. The critical point is $H = 0$ and $T = T_c$, at which we see the discontinuous onset of spontaneous magnetization.

By a similar procedure we may obtain the power law for the zero-field susceptibility, χ, near the critical point:

$$\chi \sim |T - T_c|^{-1}, \tag{1.31}$$

which diverges with critical exponent $\gamma = 1$ (in this case it is usually defined without the minus sign), in this case the same when approaching the critical point from above or below.

The mean field theory has allowed us to identify critical points of phase transitions and find their critical exponents, however we have neglected fluctuations, and with this we have lost the chance to uncover much of the physics happening at and around the critical points. Also, the mean field exponents are inaccurate in low ($d < 4$) dimensions, becoming exact in higher dimensions as each site has more nearest neighbors and hence the mean-field is closer to the actual field experienced. To go further, we need the renormalization group.

1.6 Renormalization Group

We briefly outline the process of renormalization. The renormalization group (RG) has proved to be one of the major achievements of 20^{th} century physics. Kenneth Wilson [23, 30] was the first to provide a physical picture to describe its action in the early 70's. The RG has wide applications in fields such as dynamical systems and chaos, fractals, disordered systems etc...

Critical phenomena are hard to capture through standard mean field models which neglect correlations and hence cannot explain their divergence as the transition is approached. The only way to build up a full picture of critical phenomena is to consider fluctuations over all length scales and all degrees of freedom. Hence, we turn to the RG framework to provide an understanding. The RG method takes advantage of the scale invariant, fractal physics to explain universality and predict the critical exponents.

Wilson's original formulation was based on the insight of Kadanoff who suggested that near a critical point, the correlation length is sufficiently large that averaging over groups of sites does not significantly affect the physics, just slightly modifies the parameters. By assuming the parameters transform according to the "scaling hypothesis", characteristic parameters of the critical behavior can be extracted.

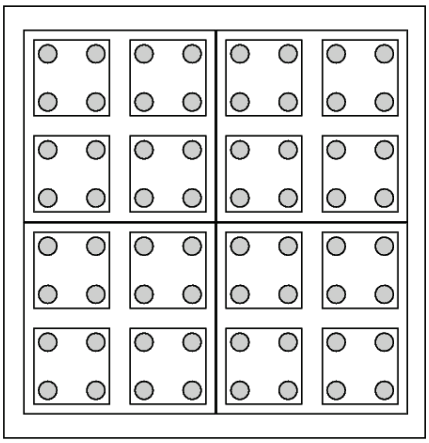

Figure 1.3: Kadanoff block spin picture on a 2d square lattice, with nearest neighbor spacing a. The lattice sites are grouped into cells of size b^2 of increasing size, such that $a < ba \ll \xi$.

1.6.1 Real Space RG for the Ising Model

Renormalization by Decimation

Take the partition function, Z, of the 1d Ising model Eq. (1.10), with N sites, in the absence of a magnetic field:

$$Z(\beta) = \sum_{\sigma} e^{-\beta \mathbf{H}(\sigma)} = \sum_{\sigma} \prod_{i} e^{K\sigma_i\sigma_{i+1}}, \tag{1.32}$$

the sum being taken over the 2^N possible spin configurations, and as usual $K = \beta J$.

Decimation involves summing over odd spins in the partition function, see Fig. 1.4. To do this, we first rewrite the partition function Z, separating out the terms for even

and odd sites, and noting that spins on odd sites do not interact directly with each other, and therefore can be summed over:

$$\begin{aligned} Z &= \sum_{\{\sigma_{2i}=\pm 1\}} \prod_{2i} \left[\sum_{\{\sigma_{2i+1}=\pm 1\}} \prod_{2i+1} e^{K(\sigma_{2i}\sigma_{2i+1}+\sigma_{2i+1}\sigma_{2i+2})} \right] \\ &= ... \\ &= \sum_{\{\sigma_{2i}=\pm 1\}} \prod_{2i} \left\{ 2\cosh\left[K\left(\sigma_{2i}+\sigma_{2i+1}\right)\right] \right\}, \end{aligned} \tag{1.33}$$

we then seek to rewrite this equation in a form similar to Eq. (1.32) but with "renormalized" coupling constant K':

$$Z = \left[\zeta(K)\right]^{N/2} \sum_{\{\sigma_{2i}=\pm 1\}} \prod_{2i} e^{K'\sigma_{2i}\sigma_{2i+2}} \tag{1.34}$$

$$= \left[\zeta(K)\right]^{N/2} Z(K', N/2), \tag{1.35}$$

where $\zeta(K)$ is the spin-independent part. Comparing Eq. (1.33) and Eq. (1.34), after some manipulations, one finds the explicit relation for the renormalized coupling constant in terms of the original coupling constant:

$$K' = \frac{1}{2}\ln(\cosh 2K). \tag{1.36}$$

This decimation procedure is repeated, and we examine the flow in parameter space of the renormalized coupling constant K. We look for the renormalized coupling constant flowing towards fixed points. Unstable fixed points are associated with the critical behavior of the model at a temperature T_c.

Figure 1.4: Decimation of 1d Ising chain, sites filled in black are summed over in the partial evaluation of the partition function.

A similar procedure can be carried out in the case of the 2d Ising model, in this case a tower of additional perturbative interactions is generated at each renormalization step, which we must take to be negligible.

1.6.2 Scaling Form

The scaling form can be used to calculate critical exponents associated with a fixed point by linearizing the RG recursion relations about that fixed point

Given a generalized recursion relationship $K_i' = R_i(K_1, K_2, ..., K_n)$, we may expand linearly around the critical point K_i^*:

$$K_i' = R_i(K_j) \simeq K_i^* + \left.\frac{dR_i}{dK_j}\right|_{K=K_i^*} (K - K_i^*) + \cdots, \tag{1.37}$$

one then calculates $\delta K_i' = K_i' - K_c^*$ and $\delta K_i = K_i - K_i^*$ and rearranges Eq. (1.37) to obtain the linearized recursion relations:

$$\delta K_i' = \sum_{j=1}^{n} \frac{\partial R_i}{\partial K_j}\Big|_{\{K_i\}=\{K_i^*\}} \delta K_j \equiv \sum_{j=1}^{n} M_{ij}\delta K_j. \tag{1.38}$$

Now, the eigenvectors and eigenvalues of the matrix $\mathbf{M}$ with elements M_{ij} may be calculated: $\mathbf{M}U_i = \lambda_i U_i = b^{y_i}U_i$, where λ_i are the eigenvalues and U_i, called the linear "scaling fields", are the corresponding eigenvectors for $i = 1, 2, ..., n$.

The singular part f_s of the free energy density f can now be written in the scaling form:

$$f_s(U_1, U_2, ..., U_n) = b^{-d} f_s(b^{y_1}U_1, b^{y_2}U_2, ..., b^{y_n}U_n), \tag{1.39}$$

where b is the linear change of scale, and d is the dimension of the system. This form of the free energy is called the "generalized homogeneous function", from which we obtain relations between critical exponents.

The scaling fields U_i are characterized as relevant if the corresponding $y_i > 0$, irrelevant if $y_i < 0$ and marginal if $y_i = 0$. Relevant scaling fields are unstable, if they are initially away from the critical point, they will move further away with renormalization, relevant quantities must therefore vanish at critical points. Irrelevant scaling fields are stable, if they are initially away from the critical point, they will move towards it with renormalization. Marginal quantities are unaffected under the action of the renormalization group.

1.6.3 Momentum Space RG for the Ising Model

The momentum space picture of a real space system is found by taking the Fourier transform, the Fourier modes become the systems degrees of freedom. The partial summation is done by integrating over short-wavelength modes, i.e. neglecting the short scale fluctuations, just as in the real space RG. We briefly review, in outline, the stages of the momentum space RG.

Ising Model as a Field Theory

In the case of the Ising model, we must first transform it into a field theory. We replace the discrete spins on a discrete lattice with continuous spins in continuous space. Firstly, recall the Hamiltonian for the Ising model without an external magnetic field H, write it in the following, slightly modified, form:

$$\mathbf{H} = -\frac{1}{2}\sum_{i,j=1}^{N} J_{ij}\sigma_i\sigma_j, \tag{1.40}$$

where the factor $1/2$ compensate for double counting of spin pairs, and the coupling constant J_{ij} is taken to be J if i and j are nearest neighbors, and zero otherwise. Now, note the following identity:

$$\exp\left(\frac{1}{2}\sum_{ij}K_{ij}\sigma_i\sigma_j\right)$$
$$=\left[\frac{\det\mathbf{K}}{(2\pi)^N}\right]^{1/2}\int_{-\infty}^{\infty}\cdots\int_{-\infty}^{\infty}\prod_{k=1}^{N}\mathrm{d}\phi_k\exp\left(-\frac{1}{2}\sum_{ij}\phi_iK_{ij}\phi_j+\sum_{ij}\sigma_iK_{ij}\phi_j\right), \quad (1.41)$$

where $\mathbf{K}$ is the matrix with elements K_{ij}. This is known as the "Hubbard-Stratonovich" transformation. Using this identity, the partition function

$$Z=\sum_{\{\sigma_i=\pm1\}}e^{\frac{1}{2}\sum_{ij}K_{ij}\sigma_i\sigma_j}, \quad (1.42)$$

can be rewritten as:

$$Z=\left[\frac{\det\mathbf{K}}{(\pi/2)^N}\right]^{1/2}\int_{-\infty}^{\infty}\cdots\int_{-\infty}^{\infty}\prod_{k=1}^{N}\mathrm{d}\phi_k$$
$$\times\exp\left\{-\frac{1}{2}\sum_{ij}\phi_iK_{ij}\phi_j+\sum_i\ln\left[\cosh\left(\sum_jK_{ij}\phi_j\right)\right]\right\}. \quad (1.43)$$

This is an exact transformation of the original partition function Eq. (1.42), but expressed in terms of continuous degrees of freedom ϕ_i at the lattice sites.

The next step is to replace the discrete lattice by a continuum in the partition function. The continuous lattice variable ϕ_i, must be replaced by a continuous function $\phi(\vec{x})$, where $\vec{x}=(x_1,x_2,...,x_d)$. Through various manipulations, and approximations we arrive at the continuum expression for the partition function as a path integral over $\phi(\vec{x})$:

$$Z=\left[\frac{\det\mathbf{K}}{(\pi/2)^N}\right]^{1/2}\int\mathcal{D}\phi(\vec{x})$$
$$\times\exp\left\{-\int\left[r\phi^2(\vec{x})-D\phi(\vec{x})\nabla^2\phi(\vec{x})+u\phi^4(\vec{x})+\cdots\right]\mathrm{d}\vec{x}\right\}, \quad (1.44)$$

where, $r=\frac{1}{2}Kz(1-Kz)$, $D=-\frac{1}{2}Ka^2(1-2Kz)$ and $u=\frac{1}{12}(Kz)^4$.

Now we have our partition function transformed into a correct form for a field theory, we can obtain equations of state by the usual derivatives of the partition function, terminating the expansion in the exponent of Eq. (1.44), as necessary (i.e. to obtain easily solvable Gaussian integrals).

RG Analysis of the Gaussian Field Theory

By terminating the expansion at 2^{nd} order in Eq. (1.44), and manipulating, we obtain the "Gaussian model" partition function (up to a constant of proportionality):

$$Z=\int\mathcal{D}\phi(\vec{k})\exp\left[-\int_0^{\Lambda}\frac{d\vec{k}}{(2\pi)^d}(r+Dk^2)|\phi(\vec{k})|^2\right], \quad (1.45)$$

where we have transformed into momentum $\vec{k}$ space, and introduced an ultraviolet cutoff Λ, where the critical quantities should not depend on this cutoff (the cutoff is equivalent to neglecting the short-scale fluctuations in the position space RG).

The momentum space RG transformation now consists of the following steps which we will see in action later on:

1. Integrating over degrees of freedom corresponding to large k (equivalent to coarse-graining blocks in the position space RG)
2. Rescaling the wavevector to restore the original range of degrees of freedom
3. Renormalization of the spin variables to restore the spatial dependence of the fluctuations

1.7 Giant Magnetocaloric Effect

The giant magnetocaloric effect (GMCE), originally discovered in $Gd_5Si_2Ge_2$ in 1997 by Pecharsky and Gschneidner [12, 31], was a milestone in the field of magnetic cooling, breathing new life into the field. Unfortunately, in $Gd_5Si_2Ge_2$, it can only be used below room temperature. The material undergoes a 1^{st} order phase transition - the magnetization changes discontinuously - strongly enhancing the induced entropy change $\Delta S^{0\to H}_{magnetic}$.

Further research has revealed other Gadolinium compounds demonstrating the GMCE, such as $Gd_5(Si_xGe_{1x})_4$, $La(Fe_xSi_{1x})_{13}H_x$ and $MnFeP_{1x}As_x$ alloys as promising alternatives. Gadolinium alloys are still considered the best materials for room temperature magnetic refrigeration as they undergo 2^{nd} order phase transitions, which have no associated hysteresis.

It was also discovered that the magnetic phase transition is accompanied by a structural deformation of the lattice, this lattice deformation leads to a change in lattice entropy which adds to the magnetic entropy change, increasing the effect [32–34] in the GMCE (alternately the lattice entropy change may decrease the effect).

It thus became important to have a theoretical model of both the magnetic and lattice degrees of freedom, what we will refer to as a "compresible Ising model". It is natural to view the magnetic lattice, to a good approximation, as a traditional Ising model, with fixed sites. However to understand the GMCE, we must extend the traditional Ising model to allow compressibility, and hence the effect of deformations of the crystal lattice.

1.8 Landau Theory of Phase Transitions for the MCE and GMCE

The Landau theory of phase transitions is a phenomenological model, useful as a general theory of 2^{nd} order phase transitions. One must assumes that the free energy is analytic at the critical point and obeys the symmetry of the the Hamiltonian.

In our case, it describes the free energy at the ferromagnetic to paramagnetic critical point. The magnetization M is chosen as an order parameter, $M = 0$ in the disordered phase, and $M \neq 0$ in the ordered phase. The free energy F is written as a general expansion at the critical point, using only even powers (to maintain global $\mathbf{Z}_2$ symmetry of the Hamiltonian in the spins), with a term for the external magnetic field interaction:

$$F(M,T) = F_0(T) + \frac{1}{2}A(T-T_c)M^2 + \frac{1}{4}BM^4 + \frac{1}{6}CM^6 - MH. \tag{1.46}$$

In this case, we have included terms up to the sixth power. We have also broken the symmetry with the last term on the right hand side which incorporates the free energy decrease when the spins align with the field.

Given particular coefficients, we can then calculate minimums of the free energy, in order to find stable states at different temperatures, equilibrium magnetizations, internal energies etc... we obtain for example, the equation of state:

$$\frac{H}{M} = A(T-T_c) + BM^2 + CM^4. \tag{1.47}$$

With positive A and B parameters, and $C = 0$, this equation is suitable for describing a simple ferromagnet.

Now we wish to use a Landau expansion for free energy that is applicable to the GMCE, hence we need to include a magneto-elastic coupling term to Eq. (1.46), in general (we delve into Landau expansions for the GMCE, in proper detail later on in section Sec. 3.6), the contribution is of the form:

$$F_{dist} = k_1 x M^2 + \frac{k_2}{2}x^2, \tag{1.48}$$

where x is the distortion between sites and k_1, k_2 are constants of the material. Minimizing this term in the distortion x, one obtains:

$$F_{dist}^{min} = -\frac{k_1^2 M^4}{2k_2}. \tag{1.49}$$

A sufficiently strong magneto-elastic coupling can induce a 1^{st} order phase transition. Hence to include the effect of lattice distortions, we include this term in the MCE landau expansion Eq. (1.46) by taking $B < 0$. As the magneto-elastic coupling gets stronger, T_c shifts to a higher temperature and we see an increased MCE.

This equation of state may be fitted to experimental results [35] with some success - Landau theory can demonstrate the GMCE resulting from magneto-elastic coupling [36]. However Landau expansions are by nature limited, being only valid near the critical point T_c, and being phenomenological, their is no clear physical interpretation of the B and C terms.

The Landau theory is a mean field theory because it does not take into account spatial fluctuation, the Ginzburg-Landau extension (originally suggested as a theory of superconductivity [37]) to the theory allows us to incorporate fluctuations, allowing us to capture much more of the physics around the critical point.

Recall that the order parameter M in the Landau theory was a constant, we now take M to be the average over a group of spins G_i (instead of all spins), in each group G_i, the local magnetization M_i is:

$$M_i = \sum_{k \in G_i} \langle \sigma_k \rangle, \tag{1.50}$$

Hence, it varies as a function of position. If the local magnetization varies slowly, we can take M_i to be continuous function of position x: $M(x)$. The Ginzburg-Landau total free energy expansion is:

$$F(M(x),T) = \int \left[F_0(T) + a(T-T_c)M^2(x) + bM^4(x) + c|\vec{\nabla}M(x)|^2 \right] \mathrm{d}x, \tag{1.51}$$

The first three terms on the right hand side generalize Eq. (1.46), the new term gives a free energy penalty for a spatially varying magnetic field.

Taking variations, we may obtain the Ginzburg-Landau equation of state:

$$H(x) = 2a(T-T_c)M(x) + 4bM^3(x) - 2c\vec{\nabla}^2 M(x). \tag{1.52}$$

2
Bean-Rodbell Model

2.1 Introduction to the Bean-Rodbell Model

Previously we had modeled the spins as an Ising model in a stationary lattice, with an exchange interaction independent of lattice spacing, which shows the usual 2^{nd} order phase transition from ferromagnetism to paramagnetism on heating. However, in real materials the exchange interaction between sites depends on lattice spacing. If we allow the lattice to deform, then it will spontaneously distort at the phase transition. The associated entropy change may act to increase or decrease the MCE depending on the parameters we will discuss below.

The magneto-elastic coupling between the magnetic and lattice degrees of freedom may be very complex, with changes in crystal symmetry, bond braking, anisotropic changes of volume etc... all possible. It is also likely that the magnetic exchange interaction is strongly dependent on the lattice deformation.

We simplify the physics by focusing on the volume change of the material, and taking the magnetic exchange energy to depend on this volume, this is the model of Bean-Rodbell [2]. To take this compressibility into account, we add to the Curie-Weiss mean field expression Eq. (3.15) the term:

$$T_c = T_0 \left(1 + \beta \left(\frac{v - v_0}{v_0}\right)\right), \tag{2.1}$$

making the critical temperature T_c dependent on volume v, where T_0 is the critical temperature of a lattice volume v_0, i.e. T_c is a linear approximation valid for small volume changes around the equilibrium volume (Fig. 2.3a). The steepness β [1] of the exchange interaction dependence on lattice spacing controls the behavior of the lattice at the critical point, and may be positive or negative. In minimizing the free energy, we will now obtain a compromise between distortion and exchange interaction.

[1] [2] and some others refer to β as the "volume strain sensitivity" of the material.

2.2 Derivation of Entropy Changes in the Bean-Rodbell Model

Following the more modern treatment found in [38], we consider the consequence of the new term Eq. (2.1) on the molecular mean field model in Sec. 3.7. We seek to theoretically derive the sign and magnitude of the lattice entropy contribution in the isothermal GMCE cycle.

2.2.1 Free Energy Expansion

We consider a generalized free energy f_L for a compressible lattice of spins, made up of contributions from the magnetic exchange interaction, the magnetic entropy S_M and and the lattice. The lattice contribution from deformations and phonons can be described by the Debye theory. The Landau free energy density of the material is:

$$f_L(M,\omega,T) = -\frac{1}{2}W(\omega)\mu_0 M^2 - TS_M(M) + f_S(\omega,T), \tag{2.2}$$

The first term being the mean field magnetic exchange energy dependent on volume by the Weiss molecular field coefficient $W(\omega)$, where $\omega = (v - v_0)/v_0$ is the reduced volume, v is the specific volume, and v_0 is the specific volume at $T = T_0$. For convenience, from now on, we will set the vacuum permeability $\mu_0 = 1$, and leave it out of expressions. The second term $-TS_M(M)$ is the magnetic entropy contribution, where M is the magnetization density. The final term $f_S(\omega,T)$ is the free energy of the structural lattice degrees of freedom.

We assume that $W(\omega)$ depends linearly on the reduced volume as $W(\omega) = W_0(1+\beta\omega)$.

It is sufficient for our aims to take the lattice free energy f_S as a power expansion of the free energy around $\omega = 0$ and $T = T_0$ [2]. First, we wish to write the reduced volume ω in terms of the pressure p combined with the isothermal compressibility $\kappa_T = -(1/v_0)dv/dp|_T$, and the temperature $T - T_0$ combined with the coefficient of thermal expansion $\alpha_p = (1/v_0)dv/dT|_p$, valid around $p = 0$ and $T = T_0$:

$$\omega(p,T) = -\kappa_T p + \alpha_p(T - T_0), \tag{2.3}$$

similarly, we write the structural entropy s_S in the form:

$$s_S(p,T) - s_0 = -v_0\alpha_p p + b_p(T - T_0), \tag{2.4}$$

where s_0 is the entropy at $T = T_0$ and $p = 0$; and $b_p = ds_S/dT|_p$ is the specific entropy capacity at constant pressure, related to the specific heat capacity at constant pressure c_p by $b_p = c_p/T$. These three independent coefficients κ_t, α_p, b_p are specific properties of the structural lattice alone, and will be taken as constants from now on. It is simple to confirm that Eq. (2.3) and Eq. (2.4) are compatible with the Maxwell relation $v_0\partial\omega/\partial T = -\partial s/\partial p$.

Recalling that in general, a Gibbs free energy $G(p,T)$ is of the form $G(p,T) = U + pV - TS$, one can obtain the structural free energy f_S that is compatible with the relations above:

$$f_S(\omega,T) = \frac{v_0}{\kappa_T}\frac{\omega^2}{2} - \left[\frac{\alpha_p v_0}{\kappa_T}\omega + s_0\right](T - T_0) - b_v\frac{1}{2}(T - T_0)^2, \tag{2.5}$$

[2] Bean-Rodbell [2] and others used the Debye formula to obtain an explicit expression for f_S.

where the first term on the right comes from the "pV" part of the free energy, the second term comes from the specific entropy capacity at constant pressure b_p, and the third term is from the specific entropy capacity at constant volume $b_v = ds_S/dT|_v = b_v - \alpha_p^2 v_0/\kappa_T$.

2.2.2 State Equations

We obtain the state equations from the total Landau free energy f_L Eq. (2.2). Using the first condition, $(1/v_0)\partial f_L/\partial\omega|_T = -p$, we obtain the equilibrium value for the reduced volume ω:

$$\omega = -\kappa_T \left(p - \frac{\eta}{3\beta\kappa_T} m^2 \right) + \alpha_p (T - T_0), \tag{2.6}$$

where $m = M/M_0$ is the reduced magnetization, and following Bean and Rodbell [2] we have introduced the dimensionless parameter η:

$$\eta = \frac{3}{2} \frac{\beta^2 \kappa_T M_0^2 W_0}{v_0}. \tag{2.7}$$

Comparing Eq. (2.6) with Eq. (2.3), we see that introducing a compressible lattice through the structural free energy f_S has introduced a new term $-\eta m^2/(3\beta\kappa_T)$ into the reduced volume ω. This term is the "exchange magnetostriction" and is due to an equivalent magneto-elastic pressure:

$$p_W = -\eta m^2/(3\beta\kappa_T). \tag{2.8}$$

Using the second condition, $\partial f_L/\partial M = H$, we obtain:

$$-W(\omega)M - T\frac{\partial s_M}{\partial M} = H, \tag{2.9}$$

substituting the equilibrium value Eq. (2.6) of the reduced volume ω, and dividing out $H_0 = M_0 W_0$, we have for $h = H/H_0$:

$$h = -\left[1 + \beta\left(\alpha_p\left(T - T_0\right) - \kappa_T p\right)\right] m - \frac{1}{3}\eta m^3 - \frac{t a_J}{n k_B}\frac{\partial s_M}{\partial m}, \tag{2.10}$$

where $h = H/H_0$, $t = T/T_{c_0}$, and

$$T_{c_0} = a_J \frac{M_0^2 W_0}{n k_B}, \tag{2.11}$$

n is the density (number per unit volume) of spins of spin quantum number J, a_J is a coefficient dependent on the magnetic moments, and k_B is the usual Boltzman constant. Rescaling, so that $T_0 = T_{c_0}$, we may rewrite the term linear in m (in Eq. (2.10) as $-[1 + \zeta(t-1) - \pi]m$. We have introduced two dimensionless parameters, the first, $\pi = \beta\kappa_T p$, and the second, most important as we will soon see is

$$\zeta = \alpha_p \beta T_{c_0}. \tag{2.12}$$

2.2.3 Magnetic Entropy

To fully evaluate Eq. (2.10), we must first evaluate the magnetic entropy $s_M(T)$. Firstly, we not that $s_M(0) = nk_B \ln(2J+1)$, where J is the total spin quantum number of the sites, this simply reflects the fact that at $T = 0$ all the spins are aligned, and their are $2J+1$ possible spin values, and hence this number of degenerate microstates at zero temperature. Next, we use the Brillouin function, $\mathcal{M}_J(x)$:

$$\mathcal{M}_J(x) = \frac{2J+1}{2J}\coth\left(\frac{2J+1}{2J}x\right) - \frac{1}{2J}\coth\left(\frac{1}{2J}x\right), \tag{2.13}$$

and use the result $-\partial s_M/\partial m = nk_B\mathcal{M}_J^{-1}(m)$ [39]. Substituting this equation, Eq. (2.13), into Eq. (2.10), we obtain:

$$h = -[1+\zeta(t-1)-\pi]m - \frac{1}{3}\eta m^3 + t_J\mathcal{M}_J^{-1}(m). \tag{2.14}$$

2.2.4 Possible Magnetization

Solving this equation for m gives us the possible stable magnetizations. To obtain the solutions, we take a power expansion, up to 3$^{\text{rd}}$ order, of the inverse function $\mathcal{M}_J^{-1}(m)$:

$$a_J\mathcal{M}_J^{-1}(m) \simeq m + b_J m^3 + \mathcal{O}(m^5) \tag{2.15}$$

where

$$a_J = \frac{J+1}{3J}, \tag{2.16}$$

$$b_J = \frac{3}{10}\frac{[(J+1)^2+J^2]}{(J+1)^2}. \tag{2.17}$$

Substituting this equation into Eq. (2.14) gives us

$$h = c_1 m + c_3 m^3 + t\mathcal{O}(m^5), \tag{2.18}$$

with $c_1 = (t-1)(1-\zeta)+\pi$ and $c_3 = tb_J - \eta/3$.

Now, we examine the possible solutions for m, depending on the values of the coefficients c_1 and c_3, and hence the possible phase transitions of the model. Firstly, note the case $h = 0$, $m = 0$, corresponding to a paramagnetic (PM) state, is always a solution. However, this is only a stable, energy minimum state, when $c_1 > 0$, i.e. $(t-1)(1-\zeta)+\pi > 0$. If $c_1 < 0$, PM is an energy maximum, but there exists a stable ferromagnetic (FM) solution, with $m < 0$.

We note that, at the temperature $t = t_p = 1 - \pi/(1-\zeta)$, we have $c_1 = 0$. Hence, we obtain the significant result, that for $\zeta < 1$ (see Eq. (2.12)), the PM state is stable for temperatures $t > t_P$.

For $\zeta > 1$, we have that unusual situation that the PM state is stable for temperatures $t < t_p$, i.e. the phase transitions is reversed, with low temperature PM and high temperature FM. Since the lattice thermal expansion α_p is generally a positive number, i.e. the material expands with increasing temperature, $\zeta > 1$ generally implies $\beta > 0$, corresponding to an exchange interaction strength increasing with distance. Hence, we can imagine as the material heats from below the critical temperature t_p, it begins in a PM state. As is heats, it expands ($\alpha_p > 0$), as it expands, the exchange interaction becomes

stronger, until crossing the phase transition into a high-temperature FM state. Taking into account the full expression for exchange interaction as a function of volume v, and not just our linear approximation, we may find that β may eventually fall back to zero, or negative, and hence the high temperature FM state, may, at high enough temperatures transform again to a PM state.

The sign of c_3 determines the order of the transition, a value of $c_3 < 0$, i.e. $\eta > 3b_J t_p$ gives a 1^{st} order transition, and a value of $c_3 > 0$, i.e. $\eta < 3b_J t_p$ gives a 2^{nd} order transition.

2.2.5 Entropy Change

Recall how we seek to maximize the MCE/GMCE by maximizing the entropy change ΔS on magnetization (for an isothermal cycle). The Born-Rodbell model now takes into account the structural lattice entropy, since we expect the material to deform on magnetization, the structural entropy change may increase (leading to the GMCE) or decrease the entropy change ΔS. We now seek to understand how entropy changes across all degrees of freedom on magnetization.

We begin by recalling that the entropy is given by $s = -\partial f_L/\partial T|_{m,\omega}$, applying this to Eq. (2.2), and using the state equation Eq. (2.6) for ω that we derived above, we have:

$$s = s_M(m) + s_W(m) + s_S(p, T), \tag{2.19}$$

where $s_M(m)$ is the magnetic entropy. We note that, the magnetic entropy $s_M(m)$ has a maximum at $m = 0$ in the PM state, and a minimum of zero at $m = 1$ (i.e. $M = M_0$) in the saturated FM state. The second term, $s_S(p, T)$ is the structural lattice entropy of equation Eq. (2.4).

The remaining term $s_W(m) = -\alpha_p v_0 p_W(m)$ is the magneto-elastic energy, it comes from the effect of the ferromagnetic exchange forces working through the magnet-elastic interaction, resulting in additional structural lattice entropy. Using Eq. (2.7), Eq. (2.8), Eq. (2.11) and Eq. (2.12), we may write the magneto-elastic entropy, $s_W(m)$ as:

$$s_W(m) = \frac{nk_B}{2a_J}\zeta m^2 \tag{2.20}$$

which again has a sign totally dependent on ζ since all the other factors are positive.

We wish to understand how the magnetic entropy, $s_M(m)$, and magneto-elastic entropy, $s_W(m)$, change on magnetization, and the relative sign between the contributions. Note that we do not need to look at the third term, the structural lattice entropy $s_S(p, T)$, which is independent of magnetization - the magneto-elastic coupling is entirely represented in the term $s_W(m)$.

If the low to hight temperature transition is 1^{st} order, the entropy increases discontinuously on heating at the transition temperature, i.e. there is an entropy jump $\Delta s = s_H - s_L > 0$, where s_H and s_L are the entropy at the high and low temperatures limits of the phase transition respectively.

Let us examine the first the case $\zeta < 1$ (low temperature FM, $m \neq 0$, to high temperature PM, $m = 0$), the magnetic entropy change is clearly positive, $\Delta s_M > 0$. Further, when $\zeta < 0$, the magneto-elastic entropy change is also positive (see Eq. (2.20)), $\Delta s_W > 0$. Hence, the two contributions have the same sign, the total entropy change Δs is greater than the magnetic entropy change alone, $\Delta s > \Delta s_M$. This enhances the MCE, giving the GMCE.

When $0 < \zeta < 1$, the magnetic entropy change Δs_M is still clearly positive, however the magneto-elastic entropy change is now negative, $\Delta s_W < 0$. There is a sign difference between the two contributions, and hence the total entropy change is small than the magnetic entropy change alone, $\Delta s < \Delta s_M$, inhibiting the MCE. The magneto-elastic coupling conspires to decrease the total entropy change over the phase transition.

For $\zeta > 1$, we have the inverted transition from low temperature PM to high temperature FM transition, and hence the magnetic entropy change on heating is negative, $\Delta s_M < 0$, but the magneto-elastic entropy change is positive, $\Delta s_W > 0$. The contributions have opposite signs, and hence the MCE is inhibited. We ask, is it possible for the magnitude of the magneto-elastic entropy change to be greater than the magnitude of the magnetic entropy change, $\Delta s_W > -\Delta s_M$, and hence achieve a positive total entropy change, $\Delta s > 0$ on heating through the phase transition despite going from low temperature PM to high temperature FM? This would still give us a possible, though inhibited MCE whereby the effect is comes from the magneto-elastic entropy change, and is inhibited by the magnetic entropy change.

We answer this question by defining the reduced entropy $\hat{s}$:

$$\hat{s} = (s_M(m) + s_W(m))/(nk_b). \tag{2.21}$$

The maximum difference between the entropies in the PM state ($m = 0$) and the saturated FM state ($m = 1$), $\Delta\hat{s}_{max} = \hat{s}(0) - \hat{s}(1)$, is

$$\Delta\hat{s}_{max} = \ln(2J + 1) - \frac{1}{2a_J}\zeta, \tag{2.22}$$

where the first term on the right hand side comes from the magnetic entropy change, and the second term comes from the magneto-elastic entropy change Eq. (2.20)

We can now see that, when $\zeta > \zeta_J = 2a_J \ln(2J + 1)$, we have $\Delta s_W > -\Delta s_M$, and therefore, since Δs_W is positive (as Δs_M is clearly negative for this transition, and we know the contributions have opposite signs), the total entropy change at the transition is positive: $\Delta s = \Delta s_M + \Delta s_W > 0$. However, the total entropy change has been reduced by the magnetic entropy change, and hence $\Delta s < \Delta s_W$.

To summarize the possible entropy changes as we go from the low to high temperature states, we have:

- $\zeta < 1$, low temperature FM to high temperature PM
  - $\Delta s_M > 0$
    - $\zeta < 0$: $\Delta s_W > 0$, $\Delta s > \Delta s_M$, GMCE
    - $0 < \zeta < 1$: $\Delta s_W < 0$, $\Delta s < \Delta s_M$, inhibited MCE
- $\zeta > 1$, low temperature PM to high temperature FM, inverse MCE
  - $\Delta s_M < 0$, $\Delta s_W > 0$
    - $\zeta > \zeta_J$: $\Delta s_W > -\Delta s_M$, $\Delta s > 0$, $\Delta s < \Delta s_W$
    - $\zeta = \zeta_J$: $\Delta s_W = -\Delta s_M$, $\Delta s = 0$
    - $\zeta < \zeta_J$: $\Delta s_W < -\Delta s_M$, $\Delta s < 0$, $\Delta s > \Delta s_M$

2.2.6 Numerical examples

Basso [38], goes on to work out numerical solutions to Eq. (2.14) with $J = 1/2$, and hence $\mathcal{M}_J^{-1}(m) = \tanh^{-1}(m)$, and also $a_J = 1$, $b_J = 1/3$, $p = 0$. Being particularly theoretically minded, we neglect to follow his working here, however we briefly present his results.

Firstly, we examine the case of $\zeta < 1$, hence a transition from FM to PM states on heating. Fig. 2.1a and Fig. 2.1b shows the magnetization m and total entropy $\hat{s}$, as a function of temperature t respectively. Values of $\eta = 2$, $\zeta = -0.5, 0.0, 0.5$, and h ranging from 0 to 0.04 in steps of 0.004 are chosen.

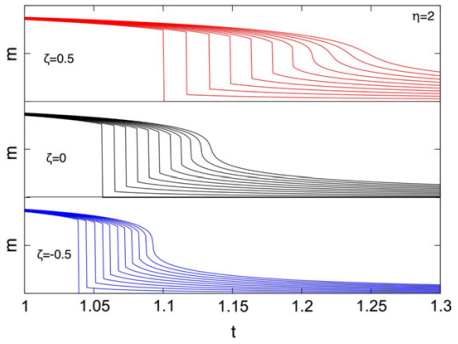

(a) Numerical solutions to Eq. (2.14) for magnetization m as a function of temperature t for several magnetic fields h from 0 to 0.04 (left to right) in steps of 0.004. $\zeta = -0.5$ (lower graph), $\zeta = 0$ (middle graph) or $\zeta = 0.5$ (upper graph).

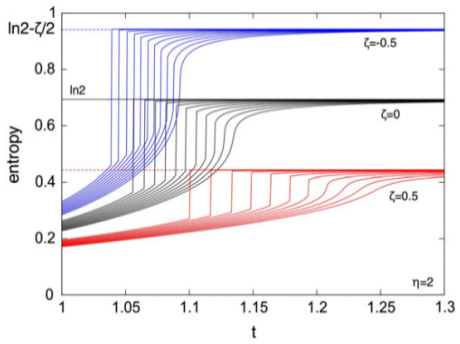

(b) Numerical solutions for total entropy $\hat{s}$ as a function of temperature t for several magnetic fields h from 0 to 0.04 (left to right) in steps of 0.004. For $J = 1/2$ the maximum entropy is $\ln 2 - \zeta/2$.

Figure 2.1: Bean-Rodbell model, numerical solutions, with FM to PM transition on heating. $J = 1/2$, $\pi = 0$ and $\eta = 2$. Graphs taken from Basso [38].

From Fig. 2.1b, we can see that the entropy change Δs increases as ζ becomes increasingly more negative and vice versa, as expected from Sec. 2.2.5. The maximum entropy change Δs for FM ($m = 1$) to PM ($m = 0$) transition is $\ln 2 - \zeta/2$ from Eq. (2.22), it is satisfying to note from Fig. 2.1b that, as expected, as we increase η, this maximum entropy change is approached.

Now, we examine the case of $\zeta > 1$, the inverted transition from PM to FM on heating. Fig. 2.2a and Fig. 2.2b shows the magnetization m and total entropy $\hat{s}$, as a function of temperature t respectively. Values of $\eta = 2$, $\zeta = 4$, and h ranging from 0 to 0.04 in steps of 0.004 are chosen.

In Fig. 2.2a, we note the unusual inverted transition is observed numerically, as we predicted theoretically in Sec. 2.2.5. Also, in Fig. 2.2b, we note the entropy change $\Delta s > 0$ on heating, since in this case, $\zeta > \zeta_J$ and hence $\Delta s_W > -\Delta s_M$. Further we note again that the total entropy change again approaches the expected limit: $\ln 2 - \zeta/2$.

2.3 Physics of the Model

Before concluding our outline of the Bean-Rodbell, we wish to have some intuitive understanding of the physics.

If we first examine $\beta > 0$, we find that the volume now changes at the new critical temperature $T_c \neq T_0$ (Fig. 2.3b) if the lattice is allowed to deform. Since the force

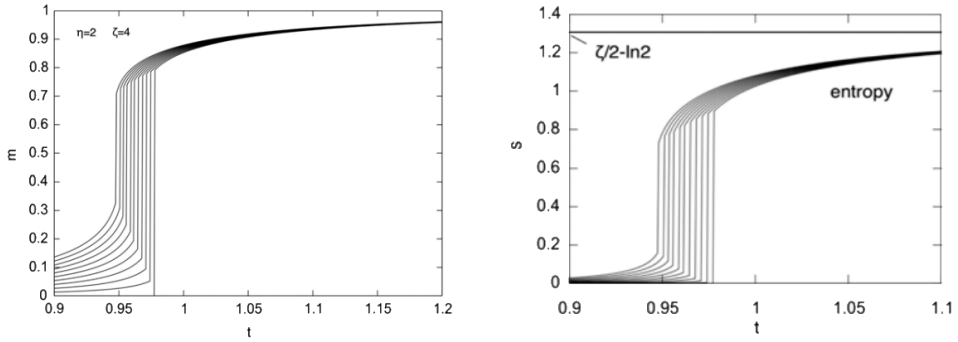

(a) Numerical solutions to Eq. (2.14) for magnetization m as a function of temperature t for several magnetic fields h from 0 to 0.04 (right to left) in steps of 0.004

(b) Corresponding numerical solutions for total entropy $\hat{s}$ as a function of temperature t. Note the maximum value of $\zeta/2 - \ln 2$ as expected.

Figure 2.2: Bean-Rodbell model, numerical solutions for the inverted transition from low temperature PM to high temperature FM states. $J = 1/2$, $\pi = 0$, $\eta = 2$ and $\zeta = 4$. Graphs taken from Basso [38].

between the sites is determined by the ordering of magnetic spins, as temperature is increased and magnetic order is lost, the force on the lattice is decreased. Above the fixed lattice critical point T_0, the magnetization will continue to decrease, but since the magnetization at these temperatures is due to the lattice deformation, which is in turn due to the magnetization, it is impossible for the magnetization to be lost continuously. Instead there must be a discontinuous step, i.e. a 1^{st} order phase transition.

In a deformable lattice, the magnetization also increases from $M = 0$ at a the new T_c (Fig. 2.3c). We can see that at low temperatures, the compressible system looses less of its magnetization than the fixed lattice because the new Curie temperature, T_c, is higher than for the fixed system, hence in a compressible Ising model, it is possible to have a ferromagnetic state at temperatures greater than the original Curie temperature, T_0, for the fixed system.

We see thermal hysteresis because on cooling the lattice distortion, which is dependent on the magnetization, does not appear until the fixed system critical point T_0. However when we heat the system back up again, the distortion increases the critical point from T_0 to T_c, and hence the magnetization is maintained until this new critical point, at which the volume and magnetization undergo a discontinuous drop to zero.

We discovered that the transition may be either 1^{st} (as in, for example [40–42], MnAs) which has been know about for a very long time) order, with the usual associated properties such as latent heat, and discontinuous density change, or 2^{nd} order depending on the value of η, a function of β and κ_p (the isothermal compressibility of the lattice), unlike the fixed-site Ising model Sec. 1.3 which shows only a 2^{nd} order phase transition.

We see that using Landau and Bean-Rodbell models, we may interpret MCE properties by fitting the models to experimental data and finding the values of coefficients. By including magneto-elastic terms coupling to the change in volume, we may include the GMCE in our models. We may use these models to better understand what temperature range provides the greatest magnetic entropy change ΔS_M, i.e. locate the peak in ΔS_M vs. T. There are however practical limitations to this approach, i.e. the mean field equations of state Eq. (3.15) and Eq. (**??**) cannot be solved analytically.

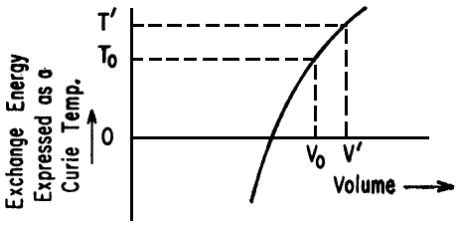

(a) Critical temperature T' as a function of volume v'.

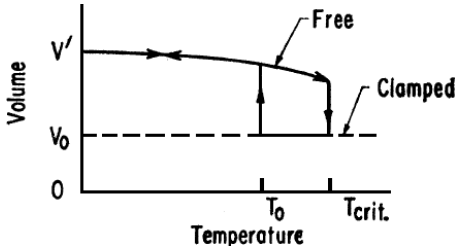

(b) Volume v' as a function of temperature T' for fixed and compressible lattices.

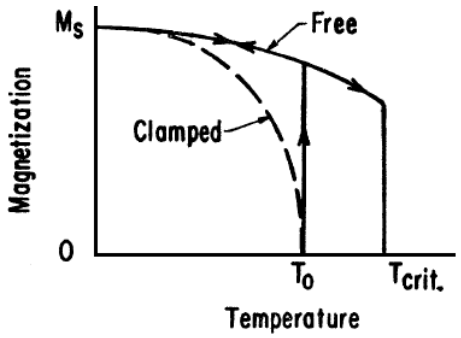

(c) Magnetization M as a function of temperature T' for fixed and compressible lattices.

Figure 2.3: Schematics of the volume dependent exchange interaction for a positive of $\beta > 0$. Graphs taken from [2].

This method may be further refined to take into account for example mixed states and material inhomogeneities [43–45], improving the fit to experimental data.

2.4 Conclusion

We have used a Landau free energy expansion to take into account both the magnetic and structural lattice degrees of freedom, and their interaction, by introducing a magneto-elastic coupling in a lattice of spins. Minimizing the free energy of the system, we calculated the total entropy change $\Delta s = \Delta s_M + \Delta s_W$ across the PM-FM phase transition and have seen that the structural contribution Δs_W may increase or decrease the magnitude of the MCE (i.e. the entropy change on magnetization) depending on the dimensionless parameter $\zeta = \alpha_p \beta T_{c_0}$, where β is the steepness of the change of exchange force with volume.

For $\zeta < 0$, the two contributions to Δs can add up, to enhance the MCE, giving rise to the GMCE. For $0 < \zeta < 1$, the two contributions have opposite sign, and hence the MCE is inhibited. Finally, for $\zeta > 1$, the structural entropy dominates, and we have an unusual inverted transition from a low temperature PM to high temperature FM state, and may have a positive or negative Δs depending on the value of ζ. Such inverted ferromagnet transitions have been observed, for example in the Ni-Mn-Sn Heusler alloy [46], and for Co-Mn-Si [47].

Hence, we have found that ζ is a very useful parameter for classifying MCE materials. Since one usually expects that $\alpha_p > 0$, the sign of ζ is usually dictated by the sign of β, we

can hence say that the GMCE is expected in materials with $\beta < 0$, i.e. the ferromagnetic exchange strength decreases with increasing volume. This is confirmed by looking at $Gd_5Si_2Ge_2$, which is a GMCE material, with experimental values from [48], Basso obtains $\zeta \simeq -0.6$, which is less than zero as expected for a GMCE material. On the other hand, for regular MCE material such as MnAs, using data from [49], Basso obtains $\zeta \simeq 0.25$, greater than zero as expected for a material only showing the MCE. In the case of MnAs, it was know from very early on that it exhibits a discontinuous loss of ferromagnetism at approximately $40°C$, with an associated latent heat, and discontinuous change of density indicative of a 1^{st} order phase transition. However, at the time (1950's), without Bean-Rodbell's theoretical understanding of entropy for a compressible spin lattice, it was thought that the transition was from ferromagnetism to anti-feromagnetism on heating. It was no until the Bean-Rodbell model, that the 1^{st} order MnAs phase transition could be explained as an FM to PM transition.

Finally, although the Bean-Rodbell model answers many of our questions, it has certain flaws. For example, we have assumed that the exchange interaction is only a function of the lattice volume, and the interaction is further assumed to be isotropic. However in reality these assumptions are incorrect, in particular they are incorrect for MnAs. This flaw in the Bean-Rodbell theory has been seen experimentally: the contraction of MnAs at critical temperature is not isotropic [41].

3

Further Theories of Compressible Ising Models

Kenneth Wilson's intuitive physical mechanism for understanding the action of the renormalization group in the early 70's (see Sec. 1.6) led to a revival of interest in the RG properties of Ising models. Hence the 70's in particular spawned several key papers in the history of compressible Ising models (CIM's). A second resurgence of interest occurred after the discovery of the GMCE in 1997, with the hope that general application of magnetic cooling technology may finally be within reach.

We review some of the key literature here, furthering our understanding of the theoretical models useful for describing the MCE/GMCE, outlining the key models (there are several more that we don't mention, less frequently encountered). In the next chapter, Ch. 4, we will get to grips with some attempts to apply RG techniques to these compressible Ising models.

3.1 General Effects of Compressibility

The standard, fixed site Ising model provides a nice picture of ferromagnetic 2^{nd} order phase transitions. It's phase diagram in the pressure-volume plane contains a transition line along which the specific heat C_v is infinite. However, it was proved by Rice [50] that such a feature in the phase space causes the system to become mechanically unstable. As a result of this, he showed that if an Ising system with divergent specific heat is put on a deformable lattice at constant pressure, it must undergo a 1^{st} order phase transition.

Hence, the standard Ising model cannot in itself be physical. To make the model more physical, one must introduce further complexities. In our case, we have introduced compressibility, via the magnetoelastic coupling. The effect of the magnetoelastic coupling is to introduce 1^{st} order transitions, which are allowed according to Rice's result.

Throughout the 70's, there was continuous debate about correctness of certain theoretical models. For example, whether or not it was necessary to include shear forces, and not just compressibility, and arguments about the physical validity of having a tricritical point in the phase space. Different models contradicted each other, a situation made much worse by the lack of experimental certainty - given that real materials never show

such sharp peaks as models predict, it was not always even possible to differentiate a 1^{st} order transition from a 2^{nd} order transition.

However the general concept that the coupling between Ising spins and lattice degrees of freedom modifies the behavior of the simple Ising model near the transition - in particular allowing a change from 2^{nd} order to 1^{st} order transition - became generally agreed upon.

3.2 Domb Model

The earliest theoretical study into the effect of compressibility on the ferromagnetic Ising system was carried out by Domb [1].

The Domb model is an Ising model on a compressible lattice where the exchange parameter J linearly depends on the average lattice spacing a. This model forms the basis for Bean-Rodbell's later mean field solution, Ch. 2, where the critical temperature T_c depends on the volume. Despite the models simplicity, it has been experimentally shown to provide order of magnitude agreement with experimental values [51].

The model takes a simple Hamiltonian containing terms for kinetic energy, quadratic potential energy and Ising terms where the exchange parameter J is a linear function of the average lattice spacing a: $J(a) = J_0 - J_1(a - a_0)$, where J_0, J_1 and a_0 are positive constants. The partition function can be factorized into an elastic part and an Ising model part:

$$Z = Z_{elastic} \times Z_I(\beta J), \tag{3.1}$$

and the free energy is:

$$F(T, a) = F_0(T) + \frac{3N}{2}\phi_2(a - a_0)^2 - \frac{1}{\beta}\log Z_I(\beta J), \tag{3.2}$$

where ϕ_2 is a positive parameter related to the compressibility, $F_0(T)$ is a smooth function of T and again $\beta = 1/(k_b T)$.

The model always predicts 1^{st} order transitions, and hence cannot explain things like lambda point transitions.

3.3 Baker-Essam Model

Baker and Essam [3] (1970) were able to solve a compressible Ising model exactly by neglecting shear forces, but accounting for nearest neighbor compression forces. Their model however does not have a 1^{st} order transition. It couples the spin Ising lattice to all the vibrational degrees of freedom, not just the uniform compression degrees of freedom in the Domb and Bean-Rodbell models.

Baker-Essam included microscopic lattice vibrations by taking a quadratic potential between sites of the form:

$$\phi(\vec{X}^{(ij)} \cdot \hat{e}^{(ij)}) = \phi_0 + \frac{1}{2}\phi_2(\vec{X}^{(ij)} \cdot \hat{e}^{(ij)} - a_0)^2, \tag{3.3}$$

where $\vec{X}^{(ij)}$ is a vector connecting lattice sites i and j, and $\hat{e}^{(ij)}$ is a unit vector from the equilibrium position of lattice sites i to j. There is a linear dependence of the exchange parameter on separation:

$$J(\vec{X}^{(ij)} \cdot \hat{e}^{(ij)}) = J_0 + J_1(\vec{X}^{(ij)} \cdot \hat{e}^{(ij)} - a_0). \tag{3.4}$$

The partition function again factorizes (in the force ensemble) into a rigid Ising model part Z_I and remaining elastic parts:

$$\log Z = \frac{3N}{2} \log\left(\frac{2\pi}{\beta\phi_2}\right) - 3N\beta\left(\phi_0 + Ka_0 - \frac{K^2 + J_1^2}{2\phi_2}\right) + \log Z_I(\beta J_{eff}), \tag{3.5}$$

in 3-dimensions, where K is the external forces and

$$J_{eff} = J_0 + J_1 K/\phi_2, \tag{3.6}$$

i.e. $Z_I(\beta J_{eff})$ is the rigid Ising model partition function calculated at an 'effective' exchange interaction strength J_{eff} - the effect of the changing lattice spacing is absorbed into this effective exchange strength for the magnetic degrees of freedom.

The relationship of the true lattice spacing a to the exchange interaction and the external force is given by:

$$a = a_0 - \frac{K}{\phi_2} - \frac{J_1}{\phi_2}\langle\sigma\sigma\rangle_{eff}, \tag{3.7}$$

where $\langle\sigma\sigma\rangle_{eff}$ is the nearest neighbor spin-spin correlation function calculated with the Ising model partition function $Z_I(\beta J_{eff})$. We see that the lattice compresses with external force - second term on the right hand side - and spin alignment - final term on right hand side.

Note that at $T = 0$, $\langle\sigma\sigma\rangle_{eff} = 1$, and hence when $K = K_0 = -\phi_2 J_0/J_1$, the lattice switches from being compressed to being expanded (see Eq. (3.7)), but more importantly the effective exchange interaction J_{eff} switches sign from being ferromagnetic to antiferromagnetic (see Eq. (3.6)) - this is the ferromagnetic to antiferromagnetic phase transition seen in the phase diagram Fig. 3.2. As the temperature is increased, both of these regions in the phase space encounter a transition to the high temperature paramagnetic phase, hence these three phase transition lines meet at the tricritical point.

Baker and Essam later extended their model by the inclusion of anti-shearing forces [52]. The model is no longer analytically solvable, but is shown to be mechanically stable, allowing 1st order transitions. The specific heat at constant volume and constant pressure have been shown to become finite at the phase transitions, however the specific heat a constant pressure remains infinite.

It is also shown to reduce to the original Baker-Essam model in the appropriate limit.

3.4 Phase Diagrams for Compressible Ising Models

Salinas [53] was the first to present and analyses the main characteristics of the phase diagrams for the compressible Ising models in zero field, of Domb (Sec. 3.2) and Baker-Essam (Sec. 3.3). These phase diagrams are particularly interesting in that they display tricritical points.

For the Domb model, the phase diagram for the 2-dimensional case is seen in Fig. 3.1. We see a pressure induced 1st order transition from antiferromagnetic to ferromagnetic state above a (negative) pressure of $-p_0 = (\phi_2 J_0)/J_1$, and at higher temperatures, above

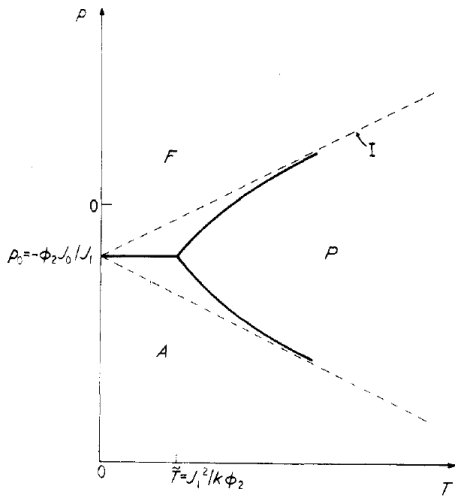

Figure 3.1: Pressure ρ vs. Temperature T phase diagram for a 2-dimensional Domb model, all the lines represent 1st order transitions. 'F', 'A' and 'P' are ferromagnetic, antiferromagnetic and paramagnetic regions respectively. Graph taken from [53].

$\tilde{T} = J_1^2/(k_B\phi_2)$, symmetric 1st order transitions from the ferromagnetic and antiferromagnetic phases to a high temperature paramagnetic phase.

For the Baker-Essam model, we see a roughly similar qualitative behavior in the phase diagram, Fig. 3.2 but with both 1st and 2nd order transitions.

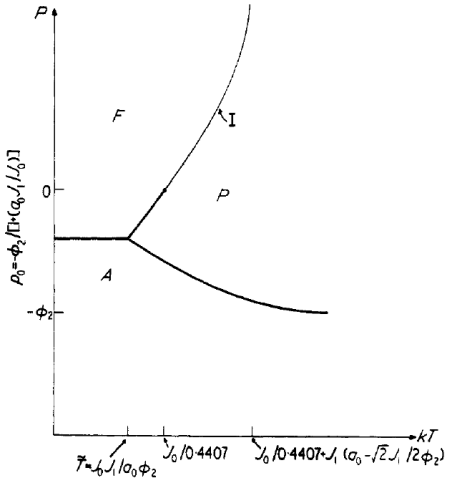

Figure 3.2: Pressure ρ vs. Temperature T phase diagram for a 2-dimensional Baker-Essam model. Lines below $\rho = 0$ are 1st order transitions, lines above $\rho = 0$ are 2nd order transitions. 'F', 'A' and 'P' are ferromagnetic, antiferromagnetic and paramagnetic regions respectively. Note the tricritical point as predicted in Sec. 3.3. Graph taken from [53].

3.5 Introducting Compression and Shear forces

The Domb, Baker-Essam and Bean-Rodbell models (as we have presented them) do not account for shear forces, only accounting for compression forces. We can attempt to

account for both using the Hamiltonian [53] (recurring indices are summed over, including those in brackets referring to a site):

$$\mathbf{H} = \Phi(\vec{X}^{(m)}) + \Psi(\vec{X}^{(m)}) + E_{KE} - \vec{K}^{(m)} \cdot \vec{K}^{(m)}, \tag{3.8}$$

where $\vec{K}^{(m)}$ are the external forces in the strain term, E_{KE} is the total kinetic energy, and where

$$\Phi(\vec{X}^{(m)}) = \sum_{<m,n>} \phi(\vec{X}^{(m)} - X^{(n)}, \tag{3.9}$$

such that Φ is the potential between sites, a quadratic function like Eq. (3.3), and the position dependent exchange interaction ψ between sites is of the form:

$$\Psi(\vec{X}^{(m)}) = \sum_{<m,n>} \left\{ -J \left[\left(\vec{X}^{(m)} - \vec{X}^{(n)} \right) \cdot \hat{e}^{(mn)} \right] \sigma_m \sigma_n \right\}, \tag{3.10}$$

such that J is a linear function like Eq. (3.4), and (mn) indicates a sum over nearest-neighbor sites only.

3.5.1 Decoupling Transformations

We can write the separation vectors in terms of the equilibrium positions, $\vec{R}^{(m)}$, and the remaining part $\vec{u}^{(m)}$: $\vec{X}^{(m)} = \vec{R}^{(m)} + \vec{u}^{(m)}$. Substituting this into Eq. (3.8), expanding, and carrying out the transformations in [53] (or as in [54–57]), we separate the effective magnetic and elastic parts to obtain:

$$\begin{aligned} \mathbf{H} = E_{KE} + \Phi(\vec{R}^{(m)}) + \frac{1}{2} v^{(m),\mu} \Phi^{(m,n),\mu\nu} v^{(n),\nu} - K^{(m),\mu} R^{(m),\mu} + \Psi(\vec{R}^{(m)} \\ + \frac{1}{2} (\Phi^{(m),\mu} + \Psi^{(m),\mu} - K^{(m),\mu} G^{(m,n),\mu\nu} (\Phi^{(n),\nu} + \Psi^{(n),\nu} - K^{(n),\nu}, \end{aligned} \tag{3.11}$$

where the terms are explained in [53], but we note here that the last term contains the so-called four-spin interaction, which in this model, is independent of the lattice spacing. This resulting Hamiltonian also contains long-range components.

3.6 Landau Theory for MCE

Amaral & Amaral [36] (following on from [58–60])in particular give an overview presentation of the effect of adding magnetoelastic and magnetoelectronic couplings to the Landau theory.

The Landau theory macroscopic free energy expansion, including even power terms upto the 6^{th} power of magnetization M, for a ferromagnetic transition, is (see Eq. (1.46):

$$F(T, M) = F_0 + \frac{1}{2} A M^2 + \frac{1}{4} B M^4 + \frac{1}{6} C M^6 - MH, \tag{3.12}$$

where the coefficients A, B and C depend on temperature, i.e. $(T - T_c)$. Energy minimization is used to obtain the magnetic equation of state:

$$\frac{H}{M} = A + BM^2 + CM^4, \tag{3.13}$$

and differentiation of the free energy Eq. (3.12) with respect to temperature gives us the magnetic entropy:

$$S_M(T,H) = -\frac{1}{2}A'(T)M^2 - \frac{1}{4}B'(T)M^4 - \frac{1}{6}C'(T)M^6, \tag{3.14}$$

where the dash indicates differentiation with respect to temperature.

In a normal ferromagnet, A, B and C, would be positive. However with the addition of the 2nd order term for magnetoelastic coupling Eq. (1.48), and its subsequent minimization Eq. (1.49), the coefficient B is decreased to a negative value. $B < 0$ gives a 1st order transition, and $B > 0$ gives a 2nd order transition in the Landau theory.

Hence for a simple ferromagnet with 2nd order transition, and $B > 0$, $S_M(T,H)$ will have a narrow peak at T_c. Further magnetoelastic contributions decrease B and broaden the peak, while leading to a much larger magnetic entropy change, $\Delta S_M(T,H) = S_M(T,H) - S_M(T,0)$, just above the critical point T_c, in Fig. 3.3.

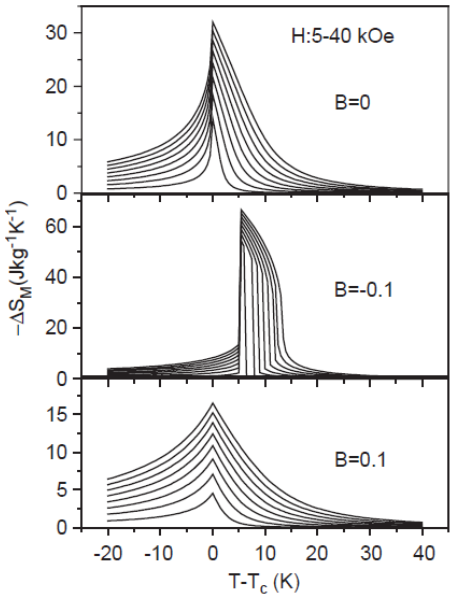

Figure 3.3: Temperature dependence of ΔS_M for positive and negative and zero B, and various values of magnetic field H. Note that for negative B, ΔS_M above the critical point becomes much larger. Graph taken from [36].

3.7 Mean Field Theory for the MCE and GMCE

To move beyond Landau theory, we look to the mean field theory. The Weiss molecular mean field theory of ferromagnetism was the first analytic treatment of 2nd phase transitions. In this theory, we consider the spins bathed in in the mean global field of the material

$$M(H,T) = M_{sat}B_J\left(\frac{H+\lambda M}{T}\right) \tag{3.15}$$

where saturation magnetization is simply taken to be $M_{sat} = Ng\mu_B J$. The Curie-Weiss law is used to estimate the (assumed constant) mean-field exchange parameter λ:

$$\lambda = T_c \frac{3k_B}{Ng^2 J(J+1)} \tag{3.16}$$

Such a simple approach does not immediately agree with experimental results, the next step is to introduce the Bean-Rodbell model [2] (or [38] for a much more modern introduction) which models 1st order transitions by considering the magneto-elastic coupling.

3.8 Insights from Monte Carlo Studies

Finally, it is worth mentioning some controversial results from Monte Carlo studies. For example, a series of papers by D. P. Landau and others [61–64] who studied the critical behavior of a 3-dimensional compressible Ising antiferromagnet at constant volume using Monte Carlo methods. In their study, they found strong indication that the system remains in the same universality class as the rigid 3-dimensional Ising model, i.e. the same critical exponents and 2nd order phase transitions are found, contrasting with the theories above. They later proved the same result using exactly the same model but with ferromagnetic interactions [65]. However they conclude that the discrepancy may be due to the finiteness of the system used in the simulation, and suggest a much larger simulation may give different results.

3.9 A Little History

We summarize the key work done on compressible Ising models during the 70's. The earliest works, leading on from Rice's result that a locus of points with a 2nd order phase transition in the phase space was unphysical, more accurately modeled real materials by including terms for magnetoelastic coupling. The effect of this on the 2nd order phase transition was not well understood until the late 70's.

First, the model by Domb appeared, which assumed the exchange interaction only depends on average lattice volume, leading to a 1st order transition. This work was extended by Bean-Rodbell (to a mean field approximation) and others. These models however were criticized for not taking into account the effect of local fluctuations of the lattice spacing on the exchange parameter J - they are all, in essence, mean field theories.

Later, Baker-Essam calculated the exact free energy for a model incorporating local distortions via an exchange interaction linearly dependent on local lattice spacing, and an potential energy quadratic in the site separation. There original model had the advantage of being exactly solvable, hence it was soon proved [66, 67] that the Baker-Essam model has a 1st order transition at negative pressure, and 2nd order transition with renormalized critical exponents for positive pressure.

Baker-Essam extended their model to include shear forces, which, although unsolvable, predicted the tricritical point would now happen at positive pressure.

Other models include the Wagner-Swift model [68] which took long-range interactions into account, this model contradicted the Baker-Essam extended model by finding no 1st order transition at positive pressures. However later investigation of this model [69] suggested it did indeed have a tricritical point at positive pressure. Another variation on Baker-Essams model was put forward by Coplan and Dresden [70], taking a cubic Ising model and adding an exchange interaction dependency to the second order in the spacing between sites, with nearest neighbors only. This model is controversial again in predicting only 2nd order transitions [71].

4

Renormalization Group Approaches to the Compressible Ising Model

We finish this thesis by examining renormalization group approaches to the compressible Ising model, in an attempt to learn more about the critical behavior at the phase transitions.

4.1 Early Approaches

One of the earliest attempts to apply RG techniques to the compressible Ising model was by Sak [72] in 1974, followed up by Bruno and Sake [73] in 1980. We follow closely their approach, specializing to the Ising model.

They considered an isotropic n-component magnet (n is the number of components in the order parameter, for the Ising model $n = 1$), with bulk modulus K_0, shear modulus μ_0 and with surfaces free to move.

We first seek to obtain recursion relations for the coupling constants in theory, then we can look to the fixed points, each of which describe a type of critical behavior. We can then obtain critical exponents by linearizing the recursion relations around each of the fixed points. Recall that relevant coupling constants for a particular fixed point are those that are unstable to small perturbations (move away from the critical point), and hence must be held at their critical values for the system to be at the critical point. Irrelevant coupling constants are stable to small perturbations (move towards the critical point), and marginal coupling constants are left unaffected by small perturbations. We note that the nature of each coupling constant (relevant/irrelevant/marginal) may be different for each critical point.

We take the dimension of the system to be $d = 4 - \epsilon$, where ϵ is originally small, allowing us to take an expansion in this parameter. Later the limit $d \to 3$ will be taken.

4.1.1 Effective Magnetic Hamiltonian

We begin by taking the Hamiltonian $\mathbf{H}$ (the Larkin-Pilkin [74] model Hamiltonian in a continuum):

$$\mathcal{H} = \frac{\mathbf{H}}{T} = \mathcal{H}_m + \mathcal{H}_e + \mathcal{H}_{em}, \tag{4.1}$$

where the magnetic part is the Ginzburg-Landau form for a rigid Ising model:

$$\mathcal{H}_m = \int d^d x \left[\frac{1}{2} r S^2(\vec{x}) + \frac{1}{2} \sum_{\alpha=1}^{d} \left(\frac{\partial S(\vec{x})}{\partial x_\alpha} \right)^2 + u_0 S^4(\vec{x}) - H S(\vec{x}) \right], \tag{4.2}$$

where r and u_0 are analytic functions of the coupling constants, H is the external magnetic field, $S(\vec{x})$ is the spin density at $\vec{x}$. The elastic part is given by [75]:

$$\mathcal{H}_e = \int d^d x \left[\left(\frac{1}{2} K - \frac{1}{d} \mu \right) \left[\vec{\nabla} \cdot \vec{u}(\vec{x}) \right]^2 + \mu \sum_{\alpha=1}^{d} \sum_{\beta=1}^{d} \left(\frac{\partial u_\alpha(\vec{x})}{\partial x_\beta} \right)^2 \right], \tag{4.3}$$

where K and μ are the bulk and shear moduli of the lattice divided by temperature T, and the field $\vec{u}(\vec{x})$ is the displacement field. The spin density $S(\vec{x})$ and the displacement field $\vec{u}(\vec{x})$ are not allowed to have spatial variations on scales smaller than the lattice spacing.

The final term in the Hamiltonian is the coupling between elastic and magnetic degrees of freedom:

$$\mathcal{H}_{em} = g \int d^d x \left[S^2(\vec{x}) \left(\vec{\nabla} \cdot \vec{u}(\vec{x}) \right) \right], \tag{4.4}$$

where the spin density is multiplied by the local compression with a coupling strength g.

We wish to construct an effective magnetic Hamiltonian $\mathcal{H}_{eff}$ for the compressible Ising model. We do this by tracing over all the elastic configurations of the system:

$$e^{-\mathcal{H}_{eff}} \equiv \mathrm{Tr}_{\vec{u}(\vec{x})} e^{-\mathcal{H}}. \tag{4.5}$$

However, first we must Fourier transform the local distortion $\partial \vec{u}(\vec{x})/\partial x_\beta$ and separate out the 0^{th} order translation mode from the periodic "phonon" modes:

$$\frac{\partial u_\alpha(\vec{x})}{\partial x_\beta} = e_{\alpha\beta} + L^{-d} \sum_{\vec{k}} i k_\beta u_{\alpha,\vec{k}} e^{i\vec{k}\cdot\vec{d}}, \tag{4.6}$$

where L is the linear size of the system (number of sites per side). The first term $e_{\alpha\beta}$ on the right hand side is the translation modes, i.e. translation of the α component of distortion u_α along the β direction. The second term is the higher order periodic modes in Fourier transformed space, where k is the wavevector, and the spin density $S(\vec{x})$ has been written as a Fourier transform:

$$S(\vec{x}) = L^{-d} \sum_{\vec{k}} S_{\vec{k}} e^{i\vec{k}\cdot\vec{x}}. \tag{4.7}$$

At this point we can impose the cutoff on fluctuations below a particular scale by limiting the range of $\vec{k}$ summed over to a sphere with radius $k = |\vec{k}|$.

Sak [73] now evaluates the Guassian integrals in the trace, Eq. (4.5), to obtain the effective Hamiltonian $\mathcal{H}_{eff}$:

$$\mathcal{H}_{eff} = \int d^d x \left[\frac{1}{2} r S^2(\vec{x}) + \frac{1}{2} \sum_{\alpha=1}^{d} \left(\frac{\partial S(\vec{x})}{\partial x_\alpha} \right)^2 + u \left(S^2(\vec{x}) \right)^2 + v L^{-d} \left(\int d^d y S^2(\vec{y}) \right) S^2(\vec{x}) - H S(\vec{x}) \right], \tag{4.8}$$

where the coupling constants are given by

$$u = u_0 - \frac{g^2}{2K} \left(1 + \frac{2\mu(d-1)}{dK} \right)^{-1}, \tag{4.9}$$

$$v = \frac{g^2}{2K} \left[\left(1 + \frac{2\mu(d-1)}{dK} \right)^{-1} - 1 \right]. \tag{4.10}$$

Looking at Eq. (4.8), we see that on the right hand side, the first term is a "mass style" term, the second is a "propogator" style term, the third is a 4 point self-interaction term. The fourth is a new interaction, generated by the procedure above, that describes interactions between magnetic degrees of freedom (spin density) at different sites on the lattice, it is a long-range interaction, mediated by the lattice itself.

Now we have our effective magnetic Hamiltonian, we can begin to study its critical behavior.

4.1.2 Critical Exponents

The RG analysis begins by finding the set of recursion relations for the coupling constants r, u, v and H. Bruno and Sak [73] do this by first Fourier transforming Eq. (4.8) to obtain:

$$\mathcal{H}_{eff} = \frac{1}{2} L^{-d} \sum_{\vec{k}} (r + k^2) S_{\vec{k}} S_{-\vec{k}} + u L^{-3d} \sum_{\vec{k}_1, \vec{k}_2, \vec{k}_3} S_{\vec{k}_1} S_{\vec{k}_2} S_{\vec{k}_3} S_{-(\vec{k}_1 + \vec{k}_2 + \vec{k}_3)} + v L^{-3d} \left(\sum_{\vec{k}} S_{\vec{k}} S_{-\vec{k}} \right)^2 - H S_{\vec{0}}. \tag{4.11}$$

They then integrate out a fraction of the degrees of freedom from the partition function, removing all $S_{\vec{k}}$ with $b^{-1} < |\vec{k}| < 1$; $b > 1$, to obtain [72] the recursion relations:

$$r' + q^2 = b^{2-\eta} \left(r + \frac{q^2}{b^2} + 12u \int \frac{d^d q}{r + q^2} + 4v \int \frac{d^d q}{r + q^2} + \cdots \right), \tag{4.12}$$

$$u' = b^{\epsilon - 2\eta} \left(u - 36u^2 \int \frac{d^d q}{(r + q^2)^2} + \cdots \right), \tag{4.13}$$

$$v' = b^{\epsilon - 2\eta} \left(v - 24uv \int \frac{d^d q}{(r + q^2)^2} - 4v^2 \int \frac{d^d q}{(r + q^2)^2} + \cdots \right), \tag{4.14}$$

(where all integrals are over $b^{-1} < |\vec{k}| < 1$). These relations are shown using Feynman diagrams in Fig. 4.1.

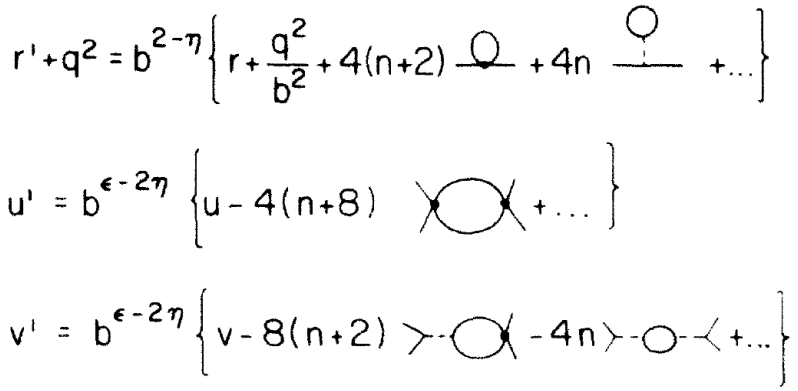

Figure 4.1: Feynman diagrams for the recursion relationships Eq. (4.12), Eq. (4.13) and Eq. (4.14). In our case (3-dimensional Ising model), $n = 1$. The 4 point self-interaction vertex u is represented by a heavy dot, the propagator for v by a dashed line, and propagator for r by a solid line. Graph taken from [72].

Examining Eq. (4.13) and Eq. (4.13) to first order in ϵ, Sak [72] finds four fixed points:

$$1) u^* = 0, \qquad v^* = 0; \tag{4.15}$$

$$2) u^* = \frac{2\pi^2}{9}\epsilon, \qquad v^* = 0; \tag{4.16}$$

$$3) u^* = 0, \qquad v^* = 2\pi^2\epsilon; \tag{4.17}$$

$$4) u^* = \frac{2\pi^2}{9}\epsilon, \qquad v^* = \frac{6\pi^2}{9}\epsilon, \tag{4.18}$$

as can be verified by substitution and some tedious algebra.

The critical exponents ϕ_u, ϕ_v and ν^{-1} of the fields u, v and r respectively, are obtained by linearization of the recursion relations in the neighborhood of the fixed points. The results are shown in Table 4.1, where instead of ν^{-1}, Sak gives $\alpha = 2 - d\nu$, and η determined from the q-dependent part of Eq. (4.12).

Fixed Point	ϕ_u	$\phi_v = \alpha/\nu$	α	η
1)	ϵ	ϵ	$\frac{1}{2}\epsilon$	0
2)	$-\epsilon + \mathcal{O}(\epsilon^2)$	$\frac{1}{3}\epsilon + \mathcal{O}(\epsilon^2)$	$\frac{1}{6}\epsilon + \mathcal{O}(\epsilon^2)$	$0 + \mathcal{O}(\epsilon^2)$
3)	ϵ	$-\epsilon + \mathcal{O}(\epsilon^2)$	$-\frac{\epsilon}{2} + \mathcal{O}(\epsilon^2)$	0
4)	$-\epsilon + \mathcal{O}(\epsilon^2)$	$-\frac{\epsilon}{3} + \mathcal{O}(\epsilon^2)$	$-\frac{\epsilon}{6} + \mathcal{O}(\epsilon^2)$	$0 + \mathcal{O}(\epsilon^2)$

Table 4.1: Fixed points and exponents to 1^{st} order in ϵ. Table taken from [72].

4.1.3 Critical Behavior

Sak [72] goes on to investigate the nature of the 4 critical points in more detail. Recall from Sec. 1.6.2, that the degree of instability of a critical point is measured by the number of positive critical exponents at that point. For example, Table 4.1 tell us that fixed point 1) is unstable in the directions of u, ν and α and marginal in the direction of η, fixed point 2) is unstable in ν and α directions, but stable the u direction etc...The projection of the

RG flow in the (u, ν) plane is give in Fig. 4.2, we note that the stable fixed point is 2), this gives the 1st order phase transition. However we note that the domain of attraction only exists for positive ν, but the system must begin in negative ν.

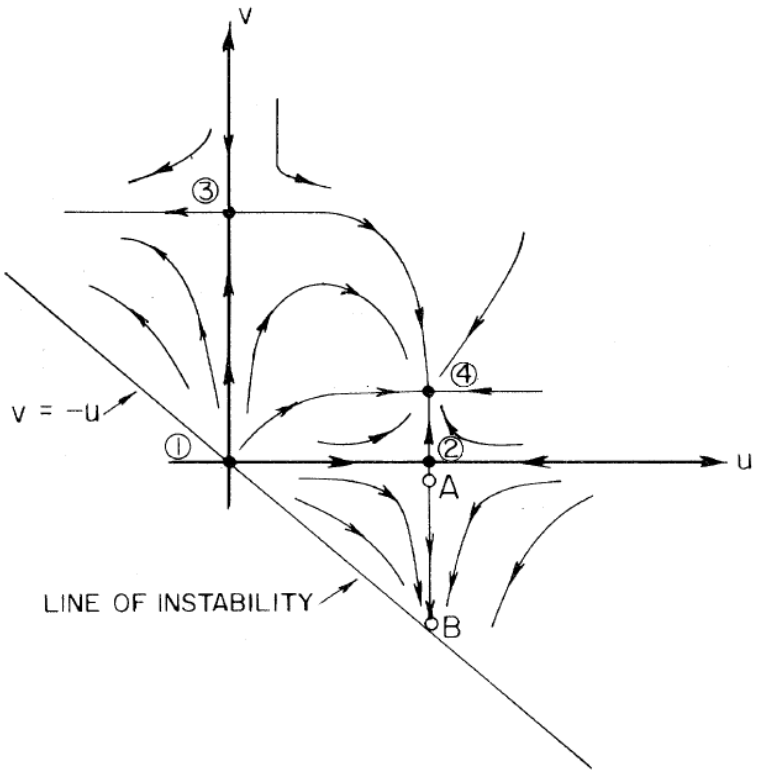

Figure 4.2: Projection of RG flow in the (u, ν) plane. Fixed points numbers as in Table 4.1. Figure taken from [73].

Bruno and Sak [73] go on to analyze this system much further. This RG technique has been successfully applied by Baker and Essam to the β-brass system [52], where they discuss further in great detail.

4.2 Further Results

In this document, we have only had time to review some of the key results of RG theory applied to compressible Ising models, there is considerably more relevant literature that we briefly note down here, so that this document may serve as a starting point for further investigation. Further results include:

Chakrabati [76] follows on from Sak [72], but treats the lattice quantum-mechanically, obtaining similar results, but with the critical point trivially accessible.

Bergman and Halperin [77] give a very thorough RG analysis of both cubic and isotropic compressible Ising models.

Two results of RG calculations [78, 79] suggest that, for a cubic lattice, any elastic anisotropy becomes increasingly important on reaching the critical point.

Aggarwal and Samathiyakanit [80] present a path integral approach to the compressible Ising model with a Wagner-Swift Hamiltonian [68], in which the exchange interaction is expanded up to terms quadratic in the displacement. They also expand their approach to the case of anharmonic crystals.

Barma and Kumar [81] attempted a position space RG approach to a Baker-Essam like compressible Ising model on various lattices. They found that the rigid Ising model fixed point was stable to weak magnetoelastic coupling, but unstable, presumably leading to a 1^{st} order phase transition beyond a critical magnetoelastic coupling (in contrast to the exact solution of the original Baker Essam model, which does not have a 1^{st} order transition, see Sec. 3.3).

Moreira, Figueiredo and Henriques [82] is a modern (2007) approach. They took a layered compressible Ising model, with ferromagnetic and antiferromagnetic couplings depending linearly on volume (as in Domb's model Sec. 3.2) then carried out an RG analysis. They find potentially accessible fixed points, with Fisher-renormalized [83] critical exponents.

Belim and Prudnikov [84] is another modern approach (2000). They tackle a similar Larkin-Pilkin style Hamiltonian to Sak's (above) approach, however their model adds frozen-in structure defects, and they examine the effects of this on a tricritical point using RG techniques. They find a significant influence from the defects.

References

[1] C. Domb, "Specific heats of compressible lattices and the theory of melting," *The Journal of Chemical Physics* **25** no. 4, (1956) 783–783.

[2] C. P. Bean and D. S. Rodbell, "Magnetic Disorder as a First-Order Phase Transformation," *Physical Review* **126** (Apr, 1962) 104–115.

[3] G. A. Baker and J. W. Essam, "Effects of lattice compressibility on critical behavior," *Physical Review Letters* **24** (Mar, 1970) 447–449.

[4] A. Kitanovski and P. W. Egolf, "Application of magnetic refrigeration and its assessment," *Journal of Magnetism and Magnetic Materials* **321** (Apr, 2009) 777–781.

[5] K. Engelbrecht, K. Nielsen, and N. Pryds, "An experimental study of passive regenerator geometries," *International Journal of Refrigeration* **34** no. 8, (2011) 1817 – 1822.

[6] "The influence of the magnetic field on the performance of an active magnetic regenerator (amr)," *International Journal of Refrigeration* **34** no. 1, (2011) 192 – 203.

[7] N. Pryds, F. Clemens, M. Menon, P. H. Nielsen, K. Brodersen, R. Bjrk, C. R. H. Bahl, K. Engelbrecht, K. K. Nielsen, and A. Smith, "A monolithic perovskite structure for use as a magnetic regenerator," *Journal of the American Ceramic Society* **94** no. 8, (2011) 2549–2555.

[8] M.-A. Richard, A. M. Rowe, and R. Chahine, "Magnetic refrigeration: Single and multimaterial active magnetic regenerator experiments," *Journal of Applied Physics* **95** (Feb, 2004) 2146–2150.

[9] M. D. Kuz'min, "Factors limiting the operation frequency of magnetic refrigerators," *Applied Physics Letters* **90** no. 25, (Jun, 2007) 251916.

[10] R. Bjrk, C. Bahl, A. Smith, and N. Pryds, "Review and comparison of magnet designs for magnetic refrigeration," *International Journal of Refrigeration* **33** no. 3, (2010) 437 – 448.

[11] J. Glanz, "Making a Bigger Chill With Magnets," *Science* **279** no. 5359, (Mar, 1998) 2045.

[12] V. K. Pecharsky and K. A. Gschneidner, Jr., "Thirty years of near room temperature magnetic cooling: Where we are today and future prospects," *International Journal of Refrigeration* **31** no. 6, (Sept, 2008) 945 – 961.

[13] K. A. Gschneidner, Jr., V. K. Pecharsky, and A. O. Tsokol, "Recent developments in magnetocaloric materials," *Reports on Progress in Physics* **68** (Jun, 2005) 1479–1539.

[14] B. G. Shen, J. R. Sun, F. X. Hu, H. W. Zhang, and Z. H. Cheng, "Recent progress in exploring magnetocaloric materials," *Advanced Materials* **21** no. 45, (Sept, 2009) 4545–4564.

[15] O. Tegus, E. Brck, L. Zhang, Dagula, K. Buschow, and F. de Boer, "Magnetic-phase transitions and magnetocaloric effects," *Physica B: Condensed Matter* **319** no. 14, (2002) 174 – 192.

[16] O. Tegus, E. Brück, K. H. J. Buschow, and F. R. de Boer, "Transition-metal-based magnetic refrigerants for room-temperature applications," *Nature* **415** (Jan, 2002) 150–152.

[17] K. G. Sandeman, "Magnetocaloric materials: the search for new systems," *ArXiv e-prints* (Jan, 2012) , `arXiv:1201.3113 [cond-mat.mtrl-sci]`.

[18] V. K. Pecharsky and J. K. A. Gschneidner, "Magnetocaloric effect from indirect measurements: Magnetization and heat capacity," *Journal of Applied Physics* **86** no. 1, (1999) 565–575.

[19] V. I. Zverev, A. M. Tishin, and M. D. Kuz'min, "The maximum possible magnetocaloric ΔT effect," *Journal of Applied Physics* **107** no. 4, (Feb, 2010) 043907.

[20] J. L. Subias, "Spin model with negative absolute temperatures for stock market forecasting," *ArXiv e-prints* (Jun, 2012) , `arXiv:1206.1272 [q-fin.ST]`.

[21] K. Huang, *Statistical Mechanics, 2nd Edition*. Apr, 1987.

[22] B. G. Nickel in *Phase Transitions: Cargese 1980*, M. Levy, J. C. Le Guillou, and J. Zinn-Justin, eds., p. 291. Plenum, New York, 1982, 1980.

[23] K. G. Wilson, "Renormalization group and critical phenomena. i. renormalization group and the kadanoff scaling picture," *Physical Review B* **4** (Nov, 1971) 3174–3183.

[24] E. Brezin, J.-C. L. Guillou, and J. Zinn-Justin, "Universal ratios of critical amplitudes near four dimensions," *Physics Letters A* **47** no. 4, (1974) 285 – 287.

[25] J. C. Le Guillou and J. Zinn-Justin, "Critical exponents from field theory," *Physical Review B* **21** (May, 1980) 3976–3998.

[26] G. S. Pawley, R. H. Swendsen, D. J. Wallace, and K. G. Wilson, "Monte carlo renormalization-group calculations of critical behavior in the simple-cubic ising model," *Physical Review B* **29** (Apr, 1984) 4030–4040.

[27] H. Blte, A. Compagner, J. Croockewit, Y. Fonk, J. Heringa, A. Hoogland, T. Smit, and A. van Willigen, "Monte carlo renormalization of the three-dimensional ising model," *Physica A: Statistical Mechanics and its Applications* **161** no. 1, (1989) 1 – 22.

[28] H. W. J. Blöte, J. A. de Bruin, A. Compagner, J. H. Croockewit, Y. T. J. C. Fonk, J. R. Heringa, A. Hoogland, and A. L. van Willigen, "Monte Carlo renormalization of the three-dimensional Ising model: the influence of truncation," *EPL (Europhysics Letters)* **10** (Sep, 1989) 105.

[29] A. M. Ferrenberg and D. P. Landau, "Critical behavior of the three-dimensional Ising model: A high-resolution Monte Carlo study," *Physical Review B* **44** (Sep, 1991) 5081–5091.

[30] K. G. Wilson, "Renormalization group and critical phenomena. ii. phase-space cell analysis of critical behavior," *Physical Review B* **4** (Nov, 1971) 3184–3205.

[31] V. K. Pecharsky and K. A. Gschneidner, Jr., "Giant Magnetocaloric Effect in $Gd_5(Si_2Ge_2)$," *Physical Review Letters* **78** (Jun, 1997) 4494–4497.

[32] V. K. Pecharsky, A. P. Holm, K. A. Gschneidner, and R. Rink, "Massive Magnetic-Field-Induced Structural Transformation in Gd_5Ge_4 and the Nature of the Giant Magnetocaloric Effect," *Physical Review Letters* **91** no. 19, (Nov, 2003) 197204.

[33] L. Morellon, Z. Arnold, C. Magen, C. Ritter, O. Prokhnenko, Y. Skorokhod, P. A. Algarabel, M. R. Ibarra, and J. Kamarad, "Pressure Enhancement of the Giant Magnetocaloric Effect in $Tb_5Si_2Ge_2$," *Physical Review Letters* **93** no. 13, (Sep, 2004) 137201.

[34] V. Pecharsky and J. Gschneidner, K.A., "Magnetocaloric effect associated with magnetostructural transitions," in *Magnetism and Structure in Functional Materials*, A. Planes, L. Maosa, and A. Saxena, eds., vol. 79 of *Materials science*, pp. 199–222. Springer Berlin Heidelberg, 2006.

[35] A. Arrott, "Criterion for Ferromagnetism from Observations of Magnetic Isotherms," *Physical Review* **108** (Dec, 1957) 1394–1396.

[36] V. S. Amaral and J. S. Amaral, "Magnetoelastic coupling influence on the magnetocaloric effect in ferromagnetic materials," *Journal of Magnetism and Magnetic Materials* **272** (May, 2004) 2104–2105.

[37] V. L. Ginzburg and L. D. Landau, "On the theory of superconductivity," *Journal of Experimental and Theoretical Physics* **50** (1950) 1064–1082.

[38] V. Basso, "The magnetocaloric effect at the first-order magneto-elastic phase transition," *Journal of Physics Condensed Matter* **23** no. 22, (Jun, 2011) 226004.

[39] C. Kittel, *Introduction to solid state physics, 5th ed.* New York: Wiley, 1976.

[40] L. F. Bates, "The Specific Heats of Ferromagnetic Substances," *Royal Society of London Proceedings Series A* **117** (Feb, 1928) 680–691.

[41] B. T. M. Willis and H. P. Rooksby, "Magnetic Transitions and Structural Changes in Hexagonal Manganese Compounds," *Proceedings of the Physical Society B* **67** (Apr, 1954) 290–296.

[42] Z. S. Basinski and W. B. Pearson, "The non-martensitic diffusionless transition in manganese arsenide at about $40°C$," *Canadian Journal of Physics* **36** (1958) 1017.

[43] L. M. Rodriguez-Martinez and J. P. Attfield, "Cation disorder and size effects in magnetoresistive manganese oxide perovskites," *Physical Review B* **54** (Dec, 1996) 15622.

[44] J. S. Amaral and V. S. Amaral, "The effect of magnetic irreversibility on estimating the magnetocaloric effect from magnetization measurements," *Applied Physics Letters* **94** no. 4, (Jan, 2009) 042506.

[45] S. Das, J. S. Amaral, and V. S. Amaral, "FAST TRACK COMMUNICATION: Handling mixed-state magnetization data for magnetocaloric studies - a solution to achieve realistic entropy behaviour," *Journal of Physics D Applied Physics* **43** no. 15, (Apr, 2010) 152002.

[46] T. Krenke, M. Acet, E. F. Wassermann, X. Moya, L. Mañosa, and A. Planes, "Martensitic transitions and the nature of ferromagnetism in the austenitic and martensitic states of $Ni-Mn-Sn$ alloys," *Physical Review B* **72** (Jul, 2005) 014412.

[47] K. Morrison, Y. Miyoshi, J. D. Moore, A. Barcza, K. G. Sandeman, A. D. Caplin, and L. F. Cohen, "Measurement of the magnetocaloric properties of $comn_{0.95}fe_{0.05}Si$: Large change with fe substitution," *Physical Review B* **78** (Oct, 2008) 134418.

[48] C. Magen, L. Morellon, P. A. Algarabel, M. R. Ibarra, Z. Arnold, J. Kamarad, T. A. Lograsso, D. L. Schlagel, V. K. Pecharsky, A. O. Tsokol, and K. A. Gschneidner, "Hydrostatic pressure control of the magnetostructural phase transition in $gd_5si_2ge_2$ single crystals," *Physical Review B* **72** (Jul, 2005) 024416.

[49] R. W. De Blois and D. S. Rodbell, "Magnetic first-order phase transition in single-crystal mnas," *Physical Review* **130** (May, 1963) 1347–1360.

[50] O. K. Rice, "Thermodynamics of Phase Transitions in Compressible Solid Lattices," *The Journal of Chemical Physics* **22** (Sep, 1954) 1535–1544.

[51] C. W. Garland and R. Renard, "Order-Disorder Phenomena. III. Effect of Temperature and Pressure on the Elastic Constants of Ammonium Chloride," *The Journal of Chemical Physics* **44** (Feb, 1966) 1130–1139.

[52] G. A. Baker, Jr. and J. W. Essam, "Statistical Mechanics of a Compressible Ising Model with Application to β Brass," *The Journal of Chemical Physics* **55** (Jul, 1971) 861–879.

[53] S. R. Salinas, "Phase diagrams for compressible Ising models," *Journal of Physics C Solid State Physics* **7** (Jan, 1974) 241–254.

[54] N. Matsudaira, "The Effect of Lattice Vibration on the Phase Transition of the Ising Model," *Journal of the Physical Society of Japan* **25** (Nov, 1968) 1225.

[55] H. Wagner, "Phase Transition in a Compressible Ising Ferromagnet," *Physical Review Letters* **25** (Jul, 1970) 31–34.

[56] H. C. Bolton and B. S. Lee, "Spin-phonon interactions in the compressible Ising magnet," *Journal of Physics C Solid State Physics* **3** (Jul, 1970) 1433–1441.

[57] B. S. Lee and H. C. Bolton, "Spin-phonon interactions in the compressible Ising magnet. II," *Journal of Physics C Solid State Physics* **4** (Jul, 1971) 1178–1192.

[58] V. Amaral, J. Arajo, Y. Pogorelov, P. Tavares, J. Sousa, and J. Vieira, "Discontinuous transition effects in manganites: magnetization study in the paramagnetic phase," *Journal of Magnetism and Magnetic Materials* **242245, Part 2** no. 0, (2002) 655 – 658.

[59] V. Amaral, J. Arajo, Y. Pogorelov, J. L. dos Santos, P. Tavares, A. Loureno, J. Sousa, and J. Vieira, "Anomalous magnetic behavior in la2/3ca1/3mno3 near the critical point: stable clusters and crossover to uniform ferromagnetism," *Journal of Magnetism and Magnetic Materials* **226230, Part 1** no. 0, (2001) 837 – 839.

[60] V. S. Amaral, J. P. Araujo, Y. G. Pogorelov, J. B. Sousa, P. B. Tavares, J. M. Vieira, P. A. Algarabel, and M. R. Ibarra, "Tricritical points in la-based ferromagnetic manganites," *Journal of Applied Physics* **93** no. 10, (2003) 7646–7648.

[61] B. Dünweg and D. P. Landau, "Phase diagram and critical behavior of the si-ge unmixing transition: A monte carlo study of a model with elastic degrees of freedom," *Physical Review B* **48** (Nov, 1993) 14182–14197.

[62] X. Zhu, F. Tavazza, D. P. Landau, and B. Dünweg, "Critical behavior of an elastic ising antiferromagnet at constant pressure," *Physical Review B* **72** (Sep, 2005) 104102.

[63] D. P. Landau, "What Do Monte Carlo Simulations Tell Us About Compressible Ising Models?," *Brazilian Journal of Physics* **36** (Sep, 2006) 640–644.

[64] L. Cannavacciuolo and D. P. Landau, "Critical behavior of the three-dimensional compressible Ising antiferromagnet at constant volume: A Monte Carlo study," *Physical Review B* **71** no. 13, (Apr, 2005) 134104, `arXiv:cond-mat/0409684`.

[65] F. Tavazza, D. P. Landau, and J. Adler, "Phase diagram and structural properties for a compressible Ising ferromagnet at constant volume," *Physical Review B* **70** no. 18, (Nov, 2004) 184103.

[66] L. Gunther, D. J. Bergman, and Y. Imry, "Renormalized Critical Behavior or First-Order Phase Transitions?," *Physical Review Letters* **27** (Aug, 1971) 558–561.

[67] D. J. Bergman, Y. Imry, and L. Gunther, "Exactly soluble magnetoelastic lattice with a magnetic phase transition," *Journal of Statistical Physics* **7** (Apr, 1973) 337–360.

[68] H. Wagner and J. Swift, "Elasticity of a magnetic lattice near the magnetic critical point," *Zeitschrift fur Physik* **239** (Apr, 1970) 182–196.

[69] N. Theodorakopoulos, "Phase transition of the compressible ising lattice," *Solid State Communications* **12** no. 9, (1973) 955 – 957.

[70] L. A. Coplan and M. Dresden, "Effects of Mechanical Stretching and Quadratic Coupling on Critical Behavior," *Physical Review Letters* **25** (Sep, 1970) 785–788.

[71] T. Ottinsen, "Quantum statistical analysis of a compressible Ising model," *Physical Review B* **10** (Nov, 1974) 3858–3863.

[72] J. Sak, "Critical behavior of compressible magnets," *Physical Review B* **10** (Nov, 1974) 3957–3960.

[73] J. Bruno and J. Sak, "Renormalization group for first-order phase transitions: Equation of state of the compressible Ising magnet," *Physical Review B* **22** (Oct, 1980) 3302–3318.

[74] A. I. Larkin and S. A. Pikin, "Phase Transitions of the First Order but Nearly of the Second," *Soviet Journal of Experimental and Theoretical Physics* **29** (1969) 891.

[75] L. D. Landau and E. M. Lifshit's, *Theory of elasticity.* 1959.

[76] B. Chakrabarti, "Critical behaviour of a compressible Ising model," *Solid State Communications* **23** (Sep, 1977) 683–685.

[77] D. J. Bergman and B. I. Halperin, "Critical behavior of an ising model on a cubic compressible lattice," *Phys. Rev. B* **13** (Mar, 1976) 2145–2175.

[78] D. J. Bergman and B. I. Halperin, "Critical behavior of an Ising model on a cubic compressible lattice," *Physical Review B* **13** (Mar, 1976) 2145–2175.

[79] M. A. de Moura, T. C. Lubensky, Y. Imry, and A. Aharony, "Coupling to anisotropic elastic media: Magnetic and liquid-crystal phase transitions," *Physical Review B* **13** (Mar, 1976) 2176–2185.

[80] K. G. Aggarwal and V. Samathiyakanit, "Path integral approach to the compressible Ising model," *Journal of Physics A Mathematical General* **8** (Feb, 1975) 226–236.

[81] M. Barma and D. Kumar, "A position space renormalisation group approach to the compressible Ising model," *Journal of Physics C Solid State Physics* **12** (Apr, 1979) 1331–1347.

[82] A. F. S. Moreira, W. Figueiredo, and V. B. Henriques, "Compressible metamagnetic model: Renormalization-group approach," *Physical Review B* **75** no. 22, (Jun, 2007) 224432.

[83] M. E. Fisher, "Renormalization of critical exponents by hidden variables," *Phys. Rev.* **176** (Dec, 1968) 257–272.

[84] S. V. Belim and V. V. Prudnikov, "Tricritical Behavior of Compressible Systems with Frozen-In Structure Defects," *Physics of the Solid State* **43** (Jul, 2001) 1353–1359.